Optimization of Processing Parameters for 3D Printed Product using Taguchi Method and Desirability Function Analysis

by

Farhana Yasmin

A Thesis

Submitted to the Faculty of Graduate Studies

University of Manitoba

in partial fulfillment of the requirements of the degree of

Master of Science

Department of Mechanical Engineering,

University of Manitoba,

Winnipeg, Manitoba

Abstract

Additive Manufacturing (AM) or 3D printing technologies use fused layers of the material to build cross-sectional geometry of product. As variable processing parameters have an impact on the product quality, it is crucial to ascertain relationships of AM process parameters, productivity, sustainability, and structure performance. This research investigates the effect of the fused deposition modeling (FDM) process parameters on the response variables including mechanical attributes, energy consumption, material consumption and manufacturing time of the 3D printed product. Experiments are conducted for the FDM variable parameters of the infill pattern, infill density, layer height, printing speed, printing temperature, and wall thickness. Design of the experiment approach is used to determine the best combination of the chosen parameters. A L18 orthogonal design method is employed to collect the testing data. Taguchi and analysis of variance methods are applied in the data analysis of variable FDM parameter settings. The research finds different effects on the response variables. The optimization of response characteristics is performed using the multi-objective optimization desirability technique. The best combinations of process parameters are obtained for the chosen response variables.

Acknowledgements

First of all, I would like to express my sincere gratitude towards my supervisor, Dr. Qingjin Peng, for his unwavering support, invaluable guidance, and expertise throughout this research. His mentorship and profound knowledge were indispensable in ensuring the successful completion of this work.

My thanks go to my parents, whose encouragement and support have been the cornerstone of my achievements. Also, I would like to acknowledge my husband, whose unwavering focus and ambition have served as a continual source of motivation. His support has propelled me forward, and I dedicate this research work to him and my little boy, Shahab Fayan Noor.

I express my gratitude to my fellow engineering students with whom I had the privilege of working and interacting. I am also thankful to the University of Manitoba for providing me with the financial support that enabled me to pursue my research work. Additionally, I would like to thank all the faculty members and personnel of the Department of Mechanical Engineering for their assistance and support in my academic endeavors. Finally, I am grateful to the Almighty for his mercy and blessings, which have allowed me to endure all the stress.

In conclusion, I'd like to take this opportunity to express my gratitude to everyone who has helped me along the way in my academic journey. Without their support, encouragement, and guidance, this thesis would not have been possible to complete.

Contents

List of Figures

List of Tables

Chapter 1

Introduction

1.1 Research background

Additive manufacturing (AM) or three-dimensional (3D) printing methods build products directly based on computer-aided design (CAD) models. AM is a revolutionary technology that enables the creation of 3D objects through the layer-by-layer addition of material. Significant benefits of AM include the fast prototyping, flexible design, and ability to produce complex and customized parts for a variety of sectors (Gibson 2015). AM grows rapidly because of its efficient digitization of production processes (Raut et al. 2014). AM has been widely used in a variety of fields, such as engineering, building, medicine, and fashion industry (Rosen 2007). Comparing with conventional subtractive manufacturing methods, AM has a lot of potential to enhance manufacturing process sustainability (Khalid and Peng 2021). Product's strength, surface quality, build time, accuracy, and repeatability are mainly based on AM process parameters, it is therefore crucial to search the best solution of setting AM parameters (Melgoza et al. 2014; Farahin et al. 2019).

There are a variety of AM methods such as fused deposition modeling (FDM), direct metal deposition (DMD), inkjet modeling (IJM), and stereolithography (SLA) (Srivastava and

Rathee 2018). Among them, FDM is a widely used and cost-effective approach to build complex 3D parts. FDM builds a part in a layer-by-layer process where thermoplastic materials are extruded through a heated printer head as shown in Figure 1.1.

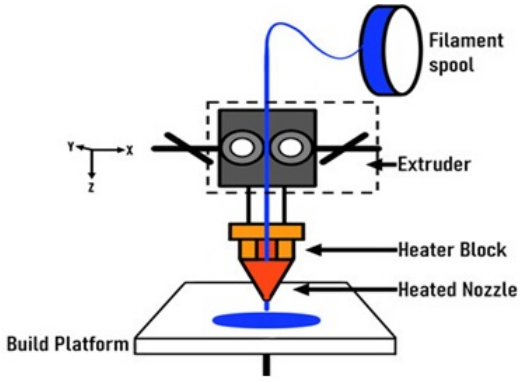

Figure 1.1: FDM process schematic diagram (Cavallo 2023).

FDM process initiates with the creation of a digital CAD model which is then converted into a stereolithographic (STL) file format (Wiedemann and Jantzen 1999) with individual layers and specific attributes such as infill percentage and wall thickness (Upcraft and Fletcher 2003). The material, typically ABS (filament) or PLA, is gradually fed into a heated extruder during the printing process. The filament used in FDM systems typically has a circular cross-section with specific diameters designed for the system. FDM process parameters include the printing layer height, number of shells, raster angle, building orientation, printing speed, infill pattern, infill percentage, infill density, printing strength, extrusion temperature, and more. These parameters have different impacts on the AM product. The energy and material consumption of the process is also considered in the process. When using the 3D printing method, crucial specifications of these parameters need to be under control, such as the product strength and surface quality (Alhubail 2012). Significant work has been conducted to improve the quality of 3D printed products, particularly in product mechanical characteristics and precision (Huang et al. 2018). Re-

searchers have investigated the effect of 3D printing parameters on part quality, building cycle, and structural performance (Mohan et al. 2017). In general, surface roughness, dimensional accuracy, material consumption, printing time, and mechanical qualities are the main characteristics of AM built parts.

Although different solutions have been proposed to select AM parameters for process efficiency and product quality (Linke 2017), there remains a research gap in developing methodologies to enhance the mechanical strength of FDM printed items. The optimal printing parameters are necessary to build high-quality and durable parts with the least time and materials. There is considerable research on the process parameters of traditional manufacturing methods, but there is a lack of research to find the effect of different parameter characteristics on AM for its energy and material consumption, and mechanical strength.

This research investigates the effects of 3D printing parameters on tensile and compression attributes of the product built by FDM. The characteristics of polylactic acid (PLA) specimens are studied using the Taguchi design of experiments approach. The Taguchi L18 Orthogonal array is formed based on 2 and 3 mixed levels of factors. Processing factor effects on response variables of the ultimate strength and modulus of elasticity and compressive stress are studied to find the optimal set of printing parameters. Material and energy consumption and printing time are also analyzed.

1.2 Research Goals

This study aims to identify critical parameter configurations that influence the output response aligning with desired manufacturing preferences. Consequently, by creating a comprehensive manufacturing process plan that provides detailed insights, FDM users can

effectively estimate the characteristics of the output response. Further experiments and parameter evaluations will contribute to the development of a knowledge system, offering recommendations for optimal process variable settings based on specific design preferences. This research explores the influence of process parameters on AM sustainability, with the goal of identifying the optimal parameters in FDM to enhance mechanical attributes of the product, such as ultimate tensile strength (UTS) and compressive strength, in following specific details.

- Searching for the optimal process parameters of the FDM process using the Design of Experiments (DOE) analysis.
- Investigating effects of 3D printing parameters on tensile and compression attributes of the product built by FDM.
- Analyzing effects of AM process parameters on the process energy consumption, material consumption and production time.
- Searching for the optimal parameter settings to enhance product quality and strength.
- Identifying parameter contributions by using the ANOVA analysis.
- Optimization of selected response variables.

1.3 Research Structure

This thesis is composed of six chapters as follows.

Chapter One is the introduction for an overview of AM, including the research scope, goals, and outlines of this thesis.

Chapter Two provides a literature review on AM, including sustainable AM parameters, Taguchi method, mechanical property analysis, and desirability function analysis.

Chapter Three outlines the methods employed in this research, such as the plan for experimentation, design of specimens, specifications of the 3D printer, control parameters and settings for printing, utilization of fused deposition modeling, material selection, techniques for measurement and testing, and implementation of desirability function analysis.

Chapter Four shows details of the experimental study and statistical analysis of the printed specimens. Optimization is searched using the desirability function analysis.

Chapter Five introduces a user interface for configuring AM parameters based on the research findings. It provides an effective tool for users to set the AM parameters.

Chapter Six summarizes the thesis work with the research conclusions, limitations of the research, and suggestions for future work. This chapter also provides an overview of the key findings and outcomes of the research.

This chapter explores the history and importance of AM. The research objectives are outlined along with the goals and objectives of this research, including optimizing printing parameters, improving product quality, and cutting manufacturing costs. In addition, it proposes a road map for navigating the research findings and outlining the thesis work.

Chapter 2

Literature Review

Additive manufacturing (AM) enables the efficient and cost-effective creation of different volumes of parts for various industries and production requirements (May 2022). AM technologies such as Stereolithography (SLA), Fused Deposition Modelling (FDM), and Selective Laser Sintering (SLS) have enabled the direct production of prototypes from CAD models. Similarly, other AM technologies utilize different processes to achieve layer-by-layer fabrication, such as curing liquid photopolymers with light, selectively melting or sintering powdered material with a laser or electron beam, jetting materials onto a build platform, or laminating and bonding sheets of material (Wong and Hernandez 2012). AM has significantly reduced the time and effort required to create prototypes, offering an efficient and streamlined approach to product development (Alhubail 2012).

AM has extensive applications across various industries such as aerospace, automobile, medical, and dental. It enables the production of stronger, lighter, and more durable parts for industry. AM offers significant advantages over traditional manufacturing techniques by eliminating steps like tooling production, parts can be produced quickly. Moreover, AM can optimize material usage for reduced waste and lower costs (Triditive 2022). However, despite its immense potential, AM still faces certain limitations that need to be

addressed for wider industry adoption. These limitations include concerns related to sustainability, reliability, productivity, robustness, material limitations, and quality (Ngo et al. 2018; Rejeski et al. 2018; Ahn 2016). As AM continues to evolve, efforts are being made to overcome these challenges and enhance the overall capabilities and suitability of AM technology for diverse industrial applications.

The optimization of AM processing parameters is widely highlighted in the literature. Simulation modeling and experimental research are commonly used to optimize AM processing parameters. A number of notable experimental techniques have been used, such as the Taguchi method, full factorial designs, ANOVA, and fuzzy logic (Selvaraj et al. 2021). These techniques highlight the variety of approaches used to maximize AM process efficiency while reducing the requirement for additional post-processing procedures.

The FDM process has drawn the interest of researchers who use various optimization strategies to improve the properties and functionality of parts. Hassanifard and Hashemi (2020) examined the effects of the raster angle and build orientation of the part on the strain-life fatigue properties of specimens made of polycarbonate (PC) with other materials. The specimens were produced in compliance with ASTM D790-17 and D638-14 specifications. The results demonstrated the effect of infill density on the mechanical characteristics of printed parts, offering important information for fine-tuning of the printing procedure to improve performance. Tanoto et al. (2017) evaluated the dimensional correctness, processing time, and tensile strength of ABS 3D printed parts. The printing plane and orientation angle were selected as the response variables analysed. It shows a considerable reduction in printing time when the part is orientated at 90° in the XZ plane. In addition to reducing printing time, this orientation improved the specimen alignment with the ASTM standard in terms of length value. According to the research Samykano et al. (2019), adjustments to certain printing parameters such as

the percentage of infill, thickness of layers, and raster angle, have a positive impact on a number of mechanical attributes, including the toughness of printed object, fracture strain, ultimate tensile strength, and elastic modulus. These results confirm that the improvement in mechanical attributes is a direct result of improvements in AM printing parameter settings.

2.1 Additive Manufacturing (AM) Technologies

Various classification systems have been proposed to categorize AM technologies. One wide classification system is from ASTM International (formerly known as the American Society for Testing and Materials) in the ASTM F2792-12 standard (Standard 2012). Based on the classification by the ASTM International Committee, AM technologies are categorized into seven different types. They are further divided into different subcategories depicted in Figure 2.1, as follows (Gibson 2015; Campbell et al. 2012; Wong and Hernandez 2012).

1. Vat Photopolymerization: It includes technologies where a liquid photopolymer resin is selectively cured by light to form the object. Examples of vat photopolymerization technologies are Stereolithography (SLA) and Digital Light Processing (DLP).

2. Material Jetting: Material jetting technologies deposit droplets of liquid material that are then solidified to create the object. PolyJet and MultiJet Modeling (MJM) are common examples of material jetting technologies.

3. Binder Jetting: A liquid binder is selectively deposited onto a powder bed to bind particles together and form the object. Metal Binder Jetting (MBJ) and Sand Binder Jetting (SBJ) are examples of binder jetting technologies.

4. Material Extrusion: The material is extruded through a nozzle or a syringe to create the object layer by layer. Fused Deposition Modeling (FDM) and Fused Filament Fabrication (FFF) fall under material extrusion technologies.

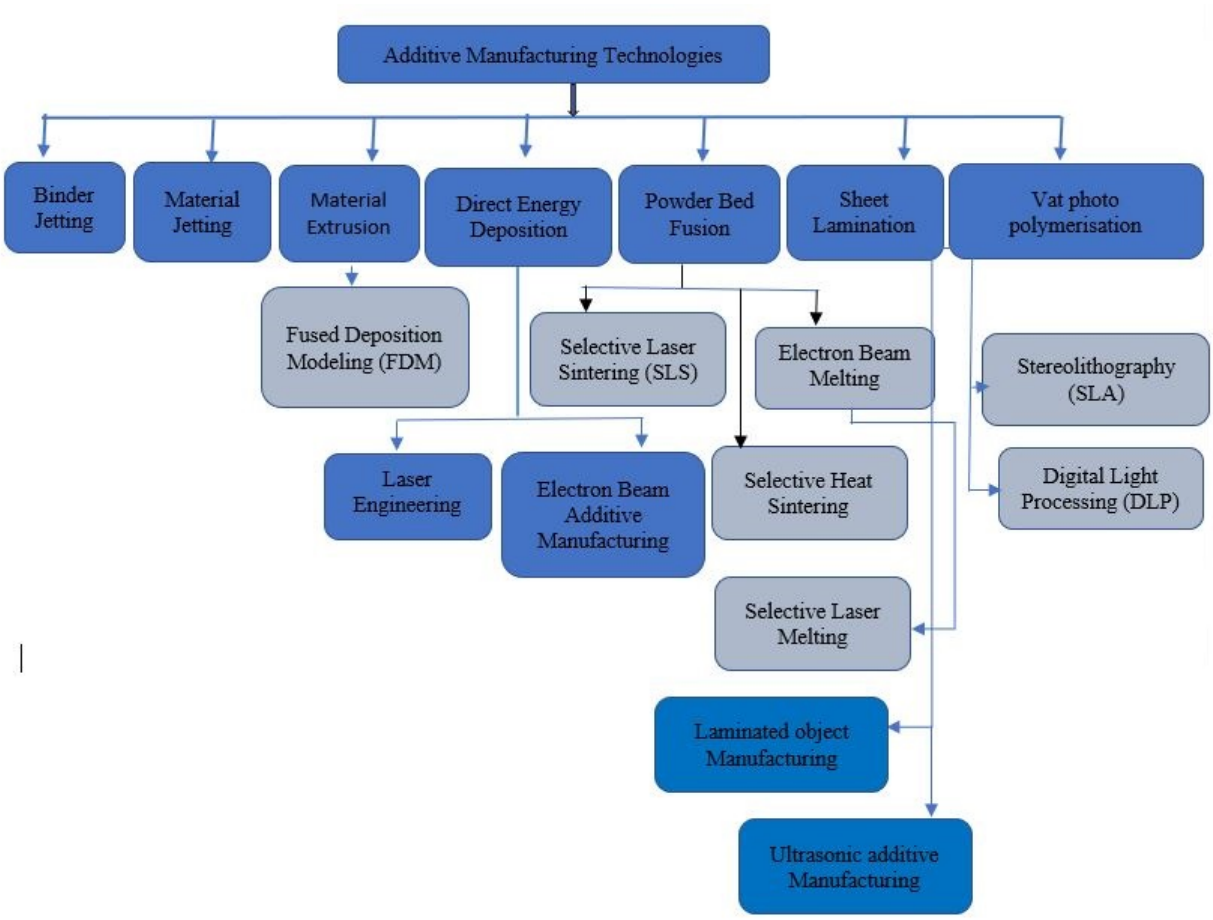

Figure 2.1: Classification for Additive Manufacturing Technologies (Rouf et al. 2022).

5. Powder Bed Fusion: It uses a laser or an electron beam to selectively fuse powdered material to create the object. Powder bed fusion (PBF) techniques melt and fuse metal powder into a solid. This technique includes: Selective heat sintering (SHS), selective laser melting (SLM), direct metal laser sintering (DMLS), electron beam melting (EBM) and selective laser sintering (SLS) (Profozich 2021).

6. Sheet Lamination: It involves layering sheets of material and bonding them together to form the object. Laminated Object Manufacturing (LOM) and Ultrasonic Additive Manufacturing (UAM) are examples of sheet lamination technologies.

7. Directed Energy Deposition: It uses focused thermal energy sources to melt and

deposit material to build up the object. These technologies are often used for large-scale AM and repair applications.

An AM process typically involves product modeling, designating printing layers and orientations, printing using appropriate building parameters, and post-processing to achieve the desired surface finish and geometry of the final object. AM approach proves particularly advantageous when creating intricate details in deep or internal surfaces, which may pose challenges for traditional subtractive manufacturing methods. The AM process involves the conversion of a digital model into physical objects through the precise deposition or solidification of materials. Different AM has its specific mechanism, materials, and processes (Gibson 2015). For example, a researcher investigated methods of directed energy deposition (DED), powder bed fusion (PBF), material extrusion (ME), and binder jetting (BJ) for the mechanical properties of materials processed (Armstrong et al. 2022).

In the material extrusion, a thermoplastic filament is fed into a heated nozzle that melts the material. The molten material is then precisely deposited onto the build platform, layer by layer, following the path defined by the sliced digital model. As each layer solidifies, the build platform moves down, allowing the next layer to be added (Wong and Hernandez 2012). Among all the AM, metal additive manufacturing (MAM) has arguably had the biggest impact on a variety of industries. For example, MAM has recently been utilized successfully in the medical field to print several surgical titanium implants (Jamróz et al. 2018).

Materials of the powder and wire are treated by melting or sintering, then solidification using hot nozzles, lasers, or electron beams (Blakey-Milner et al. 2021). Material extrusion (ME), binder jetting (BJ), powder bed fusion (PBF), directed energy deposition (DED), sheet lamination, and vat polymerization are seven major categories of MAM

processes (ISO 2015). The extensive selection of metal powders for use in AM processes is growing. Aluminum, titanium alloys, nickel, cobalt-chrome, and stainless-steel grades are a few of the most used metal materials (Profozich 2021). Not all metals can be processed using AM, though, as with many other alternative processing methods.AM research mainly addresses issues like productivity, material characteristics, and surface finishing to increase AM's potential for the industry adoption.

2.2 3D Printing Parameters

Researchers have invested in the quality of printed products, mechanical properties, and dimensional accuracy. Mechanical qualities like tensile strength are significantly impacted by AM parameters, including the build direction, layer thickness, set nozzle temperature, stability, stiffness, and Young's modulus (Ryan 2023). AM parameters affect the product quality, building cycle, and structural performance (Heidari-Rarani et al. 2022). For example, Wong and Hernandez (2012) conducted experiments and micromechanical simulations to examine the minute pores effect on material mechanical properties in the FDM process. Popescu et al. (2018) examined the mechanical characteristics of printed products for the printing settings that affect the tensile, compression, fracture, or impact strengths of the products. There is potential for a multidisciplinary approach when considering factors like printing time and machine energy consumption. In the study D'Addona et al. (2021), the desirability function was employed to optimize the filament length, product weight, and printing time. The research optimized parameters of the layer thickness, printing speed, and infill ratio for the versatility of the desirable product function.

Another research discovered that the raster layup has an effect on the final material characteristics of PLA-based FDM printed products through the analysis of the toughness,

strength, and stiffness of the product (Heidari-Rarani et al. 2022). An experiment was performed for effects of processing parameters on the mechanical characteristics and dimensional accuracy repeatability of FDM parts (Alhubail 2012). Impacts of different FDM parameters were examined including the layer thickness and raster angle. A study was conducted for the mechanical properties of FDM parts using ANOVA (Gregorian et al. 2001). An investigation was performed to find the optimal factor level for the best product quality by using the Taguchi method and Gray relational analysis (Wang et al. 2020). For the dimensional variation of printed objects, four printing parameters were used to find the optimal combination of printing parameters. The Taguchi method for optimization was paired with a fuzzy thorough evaluation (Moon 2018). A study was conducted to find the impact of the infill rate, infill pattern, and layer thickness on the dimensional accuracy of FDM. An orthogonal array L27 and a fuzzy technique were used in conjunction with the CAD model of the object to select the printing parameters (Kruth et al. 1998).

The literature consistently emphasizes the significance of printing parameters to influence the structural integrity, surface finish, and overall performance of printed parts. These parameters intricately interact to influence the structural integrity, surface finish, and overall performance of printed parts. The study also demonstrates the complex effects of parameters on 3D printed parts. However, there is a lack of research on AM parameter settings to maintain mechanical strength and reduce energy and material consumption, and time. Most of the existing research simply considers two levels of parameters or assumes linear relationships between the parameters. The relationship of product characteristics, processing energy, and material consumption requires a thorough investigation of AM processing at multiple levels to find parameter contributions for response variables.

2.3 Taguchi Method

Taguchi Method is a robust design approach to reduce variations in a process by exploring parameters' effects on the mean and variance of process performance characteristics. An orthogonal array is used to develop the experiment design (Farahin et al. 2019). Experimental factors and associated levels are chosen to form the orthogonal array. Taguchi loss functions assess performance features for measures of robustness by limiting the effects of noise components for control factors to reduce variability in the process (Wiedemann and Jantzen 1999). The signal-to-noise (S/N) ratio decides the impact of the response to the target value in various noise environments. The S/N ratio includes three categories: nominal is better, greater is better, and smaller is better (Yang and El-Haik 2009).

The Taguchi approach employs a two-step process. The first step identifies control elements to reduce variability using an S/N ratio, and the second decides control factors that move the mean toward the target with little or no impact on the S/N ratio (Cavallo 2023). The Taguchi approach is applicable in a broad range of engineering disciplines. It is useful for 'tuning' a given process for the optimal result (Khalid and Peng 2021). Taguchi orthogonal arrays have been used to confirm the impact of printing settings on the object surface roughness for the best printing parameters (Rouf et al. 2022). However, the Taguchi approach presents orthogonal arrays in a different way from those often presented in statistical literature (Devarajaiah and Muthumari 2018).

Taguchi orthogonal array design is a variant of the standard fractional factorial design approach for a set of combinations of various factors at different levels. All levels of each factor are equally considered by using balanced Taguchi orthogonal arrays. The full factorial, central composite, Box-Behnken, Plackett-Burman, Taguchi, and response surface methods are just a few of the numerous Design of Experiment (DOE) methods (Melgoza

et al. 2014). The sensitivity of each component and effects of two or more factors can be investigated using a DOE technique. DOE and Genetic Algorithms methods were applied in searching the single and multi-objective optimization with the low cost, robustness, and high effectiveness (May 2022). Different statistical and data science techniques, such as Analysis of Variance (ANOVA) and Taguchi methods, have been investigated to find the best FDM parameters that enhance the characteristics and quality of the product (Wong and Hernandez 2012). The Taguchi method provides an effective approach to finding appropriate process parameters for sustainable solutions with low energy and material costs.

2.4 Design of Experiments for Additive Manufacturing

Design of Experiments (DOE) is a method to systematically study process parameters, material compositions, and other factors in a system. DOE encompasses various techniques, including full factorial, central composite, Box-Behnken, Plackett-Burman, Taguchi, and response surface methods (Davis and John 2018). A primary objective of DOE is to design experiments cost-effectively. The choice of the appropriate DOE technique depends on objectives of the study, nature of the problem, available resources, and number of experiments and parameters to investigate. For instance, DOE has improved the quality of injection molding processes (Lin and Chananda 2003) by efficient exploring the parameter space, understanding relationships of variables, and identifying the optimal settings for desired outcomes. DOE has been used in AM to optimize process parameters, improve part quality, and enhance overall product performance by planning, conducting, and analyzing a series of experiments to efficiently explore the parameter space and identify the optimal settings. By employing DOE in AM, we can gain a comprehensive understanding of different variables that impact the final product (Elasha and Masood 2020).

Different AM process parameters like the build time, material strength, and surface roughness can be thoroughly investigated using Taguchi's DOE in Fused Deposition Modelling (FDM) (Zaman et al. 2019). Research has demonstrated considerable effects of parameters like the raster angle, air gap, and layer thickness on AM prototypes for optimizing FDM (Dakshinamurthy and Gupta 2018). Most studies examined FDM parameters on the material consumption and product strength using the multi-objective optimization for lightweight solutions (Dev and Srivastava 2020). In addition, research has explored mechanical properties of AM products, such as the tensile strength using notched bending methods and optimizations with genetic algorithms and DOE (Nguyen et al. 2020). The work improved the sample weight, printing time, and tensile strength. The application of Taguchi's DOE in Fused FDM processes offer a systematic and efficient approach to determine the optimal settings of process parameters. It can enhance the quality of FDM-produced parts while minimizing experimental trials.

The implementation of DOE in AM encompasses some sequential actions. The procedure for optimizing an AM process involves defining clear study objectives, identifying influential factors like build orientation and material composition, determining levels for each factor, designing experiments (such as full factorial or response surface designs) to explore these factors efficiently, and conducting experiments while recording relevant data. Subsequently, statistical analysis techniques like ANOVA and regression are commonly used to interpret data, uncover relationships between factors and outcomes, and finally, optimization techniques are employed to identify the optimal process parameters that align with the desired objectives, whether it's improving part quality, reducing defects, or maximizing mechanical properties (Ituarte et al. 2015).

Among the various methods used for process optimization, Taguchi's DOE enables the determination of the best combinations of process variables and their interaction effects

for desired objectives (Peace 1993). Taguchi DOE is simple, effective, and reliable in reducing costs and improving quality. It can significantly reduce the number of experiments compared to other DOE methods (Roy 2010). Through the use of Taguchi DOE, the best process parameter settings can be found and explored to increase operational efficiency and cost-effectiveness.

2.5 Mechanical Properties

Mechanical properties are essential characteristics of material behaviors under applied forces or loads. These properties play a crucial role in determining the material's suitability for specific applications and its overall performance. Mechanical properties of a material can be influenced by factors such as composition, processing techniques, heat treatment, and manufacturing defects. The field of material science has witnessed significant advancements, leading to the development of photopolymers and thermoplastics with enhanced yield strength. As a result, the use of these materials has contributed to improved part performance and durability (Griffiths et al. 2016). Over the past few years, researchers have investigated the impact of 3D printing parameters on FDM to enhance the quality of printed parts, reduce printing time, and ensure consistent structural performance (Rouf et al. 2022).

A study analyzed the tensile and flexural behaviors of ABS P400 specimens along with their processing time (Raut et al. 2014). The variable investigated was the orientation of the printed piece on the build platform. It was found that this parameter had a notable influence on all the variables studied, indicating its significant impact on the outcomes. Another research investigated the impact of build parameters on the flexural characteristics of the FDM process (Mohan et al. 2017). The study analyzed the different

build parameters influence for the flexural properties of printed parts.

While quality characteristics such as tensile strength, ductility, dimensional accuracy, surface roughness, and production time are critical considerations, it remains challenging to establish universally optimal conditions for different materials and parts. As a result, adjusting settings and parameters is an ongoing requirement to achieve desired outcomes in AM processes. With the continuous advancements in materials and technology, there is a growing possibility to manufacture not only prototypes but also functional parts using the FDM process. However, several key improvements are necessary for FDM to evolve into a viable manufacturing method for components. One crucial aspect is the enhancement of the mechanical properties of the produced parts for their structural integrity throughout their service life.

2.5.1 Tensile Properties

Tensile properties are important for the material to respond to tensile forces for its strength, ductility, and overall mechanical behavior. In FDM, the tensile properties of printed parts can vary based on various factors, including the material used, printing parameters, and post-processing techniques (Wang et al. 2020). Additionally, standards organizations such as ASTM International (American Society for Testing and Materials) and ISO (International Organization for Standardization) provide guidelines and standards for testing the tensile properties of materials, including those produced through AM processes like FDM. These standards, such as ASTM D638 and ISO 527, outline procedures and parameters for conducting tensile tests on various materials, allowing for reliable and comparable characterization of their tensile properties (ASTM-D638-14 2022). Table 2.1 displays the tensile strength of various AM systems utilizing different materials.

Table 2.1: Tensile strength of AM systems for different materials.

Material	Additive Manufacturing System	Tensile Strength (MPa)	Source
PLA	FDM	45-60	Wang et al. 2020
ABS	FDM	30-50	Huang et al. 2018
Nylon	SLS	40-60	Kruth et al. 1998
Titanium	DMLS	900-1000	Wang et al. 2019
Stainless Steel	SLM	600-800	Yadroitsev and Smurov 2010
Carbon Fiber Composite	FFF	80-120	Cuan-Urquizo et al. 2019

The tensile strength of AM systems can vary depending on the utilized materials. Different materials exhibit varying levels of tensile strength when processed using AM technologies. The information presented in the table shows the diverse range of tensile strengths achieved through different AM processes and material selections. Tensile testing is one of the most important mechanical experiments to evaluate product quality. Based on the stress/strain curves, the tensile strength and tensile modulus of the mechanical part can be decided. Tensile stress is a parameter related to stretching or tensile forces. It causes the material to elongate along the axis of the applied load. Megapascals (MPa) is the unit of measurement, and all stress values are determined using the test specimen's original cross-sectional area. The following tensile properties are decided through the tensile test (ASTM-D638-22 2022).

Elastic modulus: or the tensile modulus, is a measure of material's stiffness. When the deformation is entirely elastic, it is defined as the ratio of stress to strain. Using the stress-strain curve, elastic modulus can be decided.

UTS (ultimate tensile stress): is the highest stress that a material can withstand when a force is applied. The materials crack when they are stretched beyond their UTS. In Figure 2.2, Point B represents the point of ultimate tensile stress.

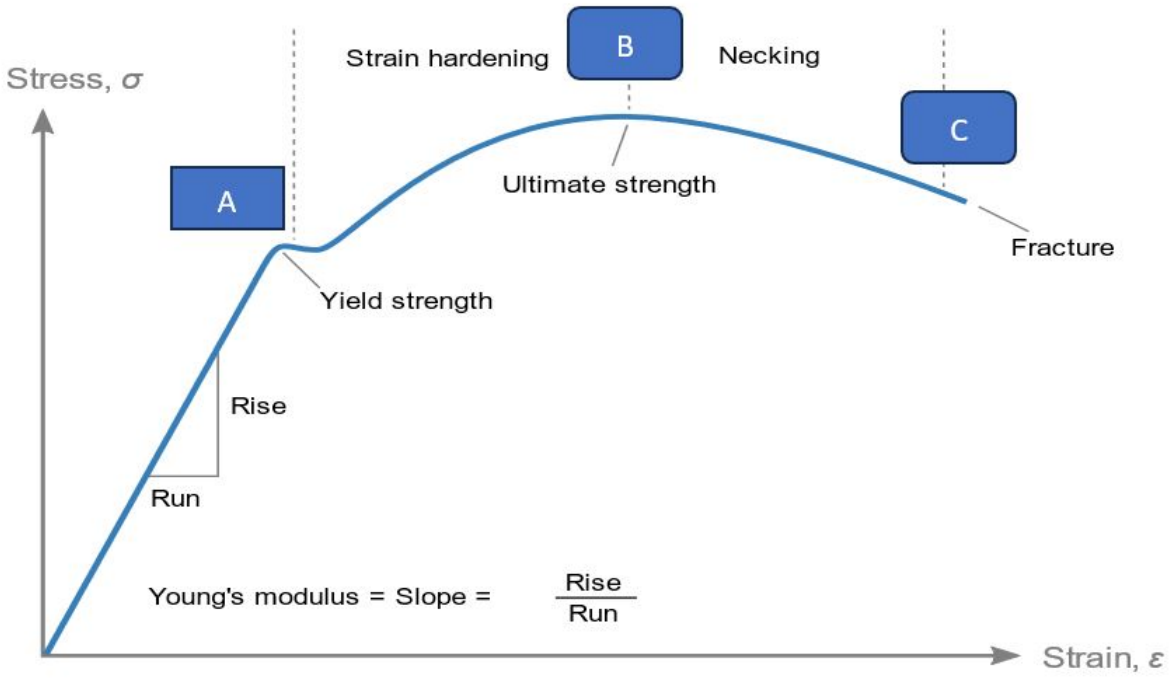

Figure 2.2: Stress - Strain curve (Wiki 2023b).

2.5.2 Compressive Properties

Compressive strength is the maximum stress that a material can withstand under compression before it fails or fractures. Compressive properties include a wide range of attributes such as modulus of elasticity, yield stress, deformation beyond the yield point, and compressive strength (unless the material undergoes flattening without fracturing). However, materials with low ductility may not exhibit a distinct yield point. In the case of materials that fail in compression due to shattering fractures, the compressive strength can be precisely determined (Yadroitsev and Smurov 2010). Conversely, for materials that do not fail in compression by shattering, the compressive strength becomes arbitrary, depending on the degree of distortion considered as a complete failure. In instances where plastic materials deform continuously in compression without a well-defined fracture, they can

eventually form a flat disk while the compressive stress steadily increases. In such cases, the compressive strength loses practical significance (ASTM-D695-23 2023).

The behavior of FDM materials in compression may differ from other materials, especially in terms of deformation and fracture characteristics. Some FDM materials may exhibit continuous deformation without a well-defined fracture point (May 2022). Although FDM materials are not subject to any specific standards for compression testing, it is beneficial to follow any applicable general standards, such as ASTM D695 or ISO 604 (ASTM 1898). These standards offer valuable guidance on the specimen preparation, test condition, and data analysis for conducting compression tests. Table 2.2 presents the compressive strength of various materials when processed using AM.

Table 2.2: Compressive strength of AM systems for different materials.

Material	AM System	Compressive Strength (MPa)	Reference
PLA	FDM	30-70	Akhoundi et al. 2019
ABS	FDM	40-90	Berman 2012
Nylon	SLS	50-100	Zhang et al. 2013
Titanium	DMLS	800-1200	Tammas-Williams et al. 2017
Carbon Fiber Composite	FFF	80-150	Kusumaatmaja et al. 2013

The compressive strength values can vary depending on factors such as specific material formulations, printing parameters, and post-processing treatments. This research will find factors that affect compressive stress.

2.6 Desirability Function Analysis

Desirability function analysis is a statistical technique to evaluate and optimize multiple response variables simultaneously. It allows to combine individual response variables into

a single desirability score, which represents the overall desirability or goodness of a system being studied. Desirability function analysis is commonly used in fields such as engineering, manufacturing, product development, and quality improvement. It considers multiple factors and finds an optimal solution to maximize the system desirability (Harrington 2006).

The multi-response characteristics are transformed into single-response features by the desirability function analysis, which searches for a single-response feature known as the composite desirability instead of complex multi-response characteristics. Achieving optimal process parameters in machining operations is crucial for product quality and performance. However, relying on a single set of parameters that satisfy a specific performance criterion often results in quality trade-offs. This is generally unacceptable as it can lead to a compromise in various performance measures. The simultaneous optimization of multiple responses becomes imperative (Devarajaiah and Muthumari 2018).

Therefore, the significance of simultaneous multi-response optimization is explored in AM processes parameters. Single-criterion optimization may result in quality compromises. Simultaneous optimization of multiple responses addresses these challenges by seeking a parameter set that achieves the best balance between various performance criteria (Dolata et al. 2020). This approach ensures that no single aspect of product quality is sacrificed for another, leading to superior overall results. Various optimization techniques are employed for this purpose, including genetic algorithms (GAs), particle swarm optimization (PSO), ant colony optimization (ACO), Grey relational analysis (GRA), desirability function analysis (DFA) (Sharma et al. 2021). DFA combines various performance criteria into a single desirability function to simplify the multi-response optimization.

A process is unsatisfactory in the desirability function analysis (DFA) method if it

contains any one of the responses that go beyond some predetermined boundaries. A set of optimum parameter settings can be found to produce the best possible individual response. All qualitative traits are transformed into [0 1] for a desirability index for each individual. Each set of response variables weighted geometric means are utilized for the desirability index. To provide the most desirable quality features under consideration, data sets with the highest composite desirability are regarded as the optimum parameter settings (Devarajaiah and Muthumari 2018). This approach is particularly useful when dealing with conflicting or competing objectives, as it provides a comprehensive evaluation for multiple criteria simultaneously. By assigning desirability values to different levels of each response variable, DFA quantifies the desirability of different combinations of parameters (Gohil et al. 2019).

The main purpose of DFA is to transform multiple responses into a single composite measure of desirability. This allows for a comprehensive evaluation of different factor combinations and facilitates the identification of the best settings for factors considered. DFA can be applied in various fields and industries where multiple criteria or objectives need to be considered. Common areas of DFA applications are as follows (Montgomery 2017):

- Product and process optimization: to optimize manufacturing processes, product designs, and material formulations by considering multiple performance criteria simultaneously.

- Quality improvement: to identify the optimal process settings for products with improved quality characteristics, such as higher strength, better surface finish, or lower defect rates.

- Experimental design: For the design and analysis of experiments by incorporating multiple response variables and determining the most desirable combination of

factor settings.

- Decision-making: to evaluate and compare alternative solutions or options based on desirability for informed decision-making.

Desirability function analysis (DFA) can effectively balance and optimize multiple criteria, leading to improved process efficiency, enhanced product performance, and overall quality enhancement (Liu et al. 2020). It is used in AM specifically to optimize process parameters by identifying the best parameter values. This method allows for the concurrent evaluation of several variables to identify the best parameter settings for AM results.

This chapter reviews the existing research on additive manufacturing (AM) to explore different topics of AM, such as AM process parameters for sustainability, Taguchi method, design of experiments, analysis of mechanical properties, and desirability function analysis.

Chapter 3

Research Methods

This chapter provides an overview of the methods and techniques utilized to conduct the research. It shows a roadmap of the methodical techniques used to collect, analyze, and interpret data, including a framework of the research, design of the experiment, and data collection methods to address the research problems.

3.1 Research Framework

Four key FDM process responses are investigated, including the printing time, energy consumption, material used, and mechanical properties of specimens through tensile and compressive tests. Experiments are designed to examine variable factors to enhance features or forecast outcomes of the FDM process. Steps of the experiment are set out step by step. Levels and choices of the FDM process parameters are investigated based on ways they might be used in the process. Design of Experiment (DOE) methods are used to assess the impact of various parameter-level combinations on outputs. Following measurements and testing of specimens, a statistical analysis of the collected outcome data is performed to search the optimal parameters for the FDM process and their interactional effects on the desired characteristics defined in this study. The process flowchart is described in

Figure 3.1.

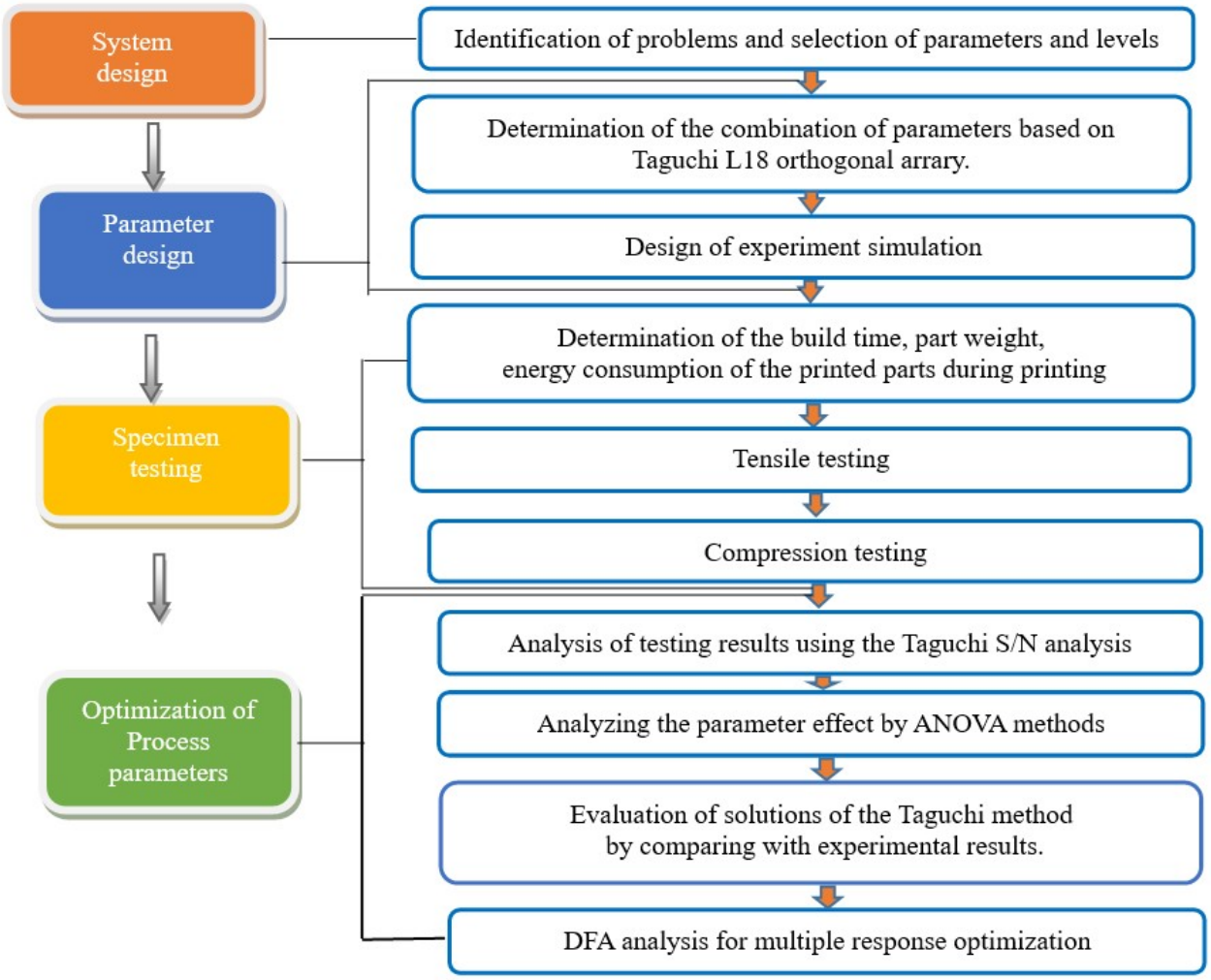

Figure 3.1: Flowchart of the method.

As shown in Figure 3.1, the system design phase begins with the identification of research problems and the choice of parameters and levels to find the optimum solutions for FDM in the energy use and material consumption, printing time along with the tensile and compressive attributes. The second stage selects the combination of parameters in the Taguchi L18 orthogonal array. The third stage designs the experiment and gathers data from tests. The following stages are printing experimental specimens and performing tensile and compression experiments. The final phase is the optimization of the process parameters.

Throughout these stages, data are examined using the Taguchi S/N analysis to determine optimal parameter settings, and interactions. ANOVA analysis is performed to find out the parameter effects on responses and determine the best parameter settings. To verify the outcome of the Taguchi method, experiments are conducted to compare the predicted values. Finally, Desirability Function Analysis (DFA) is executed to optimize all the chosen response variables.

3.2 Specimen Design

Tensile and compression tests are used for mechanical experiments to evaluate FDM product quality. By extrapolating the stress/strain curves, the strength and modulus of the tested specimens can be decided. Two types of specimens for tensile and compression tests are designed based on the ASTM standard dimensions as shown in Figure 3.2. In ASTM standards for tensile testing, the dogbone design refers to a specific shape of the test specimen used for conducting tensile tests as shown in Figure 3.2 (a). The dogbone shape is commonly employed in materials testing to evaluate the mechanical properties. A cubic sample is deigned with a side length of 19.75 mm is shown Figure 3.2 (b) for the compression test.

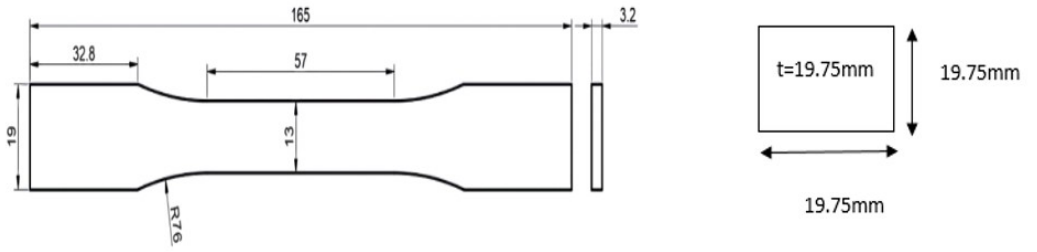

(a) Tensile specimen (b) Compression specimen

Figure 3.2: Specimens (in mm).

3.3 3D Printer Specifications

The specimens are produced using a Creality Ender 3D printer shown in Figure 3.3.

The Ender 3 has an open-frame design, which makes it easy to access and observe the printing process. Specifications of the 3D printer are shown in Table 3.1. Samples for tensile and compression testing are modeled in SolidWorks and converted into the stereolithography (STL) file format. The models are sliced using the Creality software tool before 3D printing, and then printed using 1.75 mm diameter PLA material.

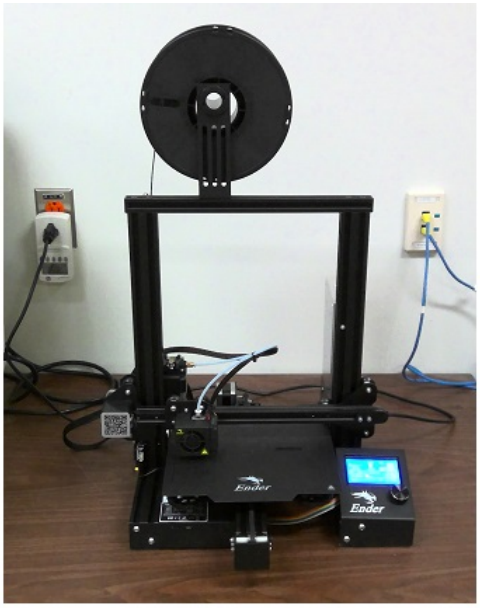

Figure 3.3: Ender Pro 3 printer.

Figure 3.4 depicts a simulation of the printing procedure. The Creality software tool is also used to set up printing parameters. Additionally, it offers a simulated preview of the time required and the energy consumption expected during the printing process. This simulation allows users to estimate the duration and energy usage associated with the 3D printing samples before the actual printing begins. The printing time for each sample is measured using a stopwatch and by the Ender Pro 3 printer. The stopwatch starts

measuring the time when the printing nozzle starts moving, whereas the Ender printer starts measuring when the nozzle and printing bed start to heat up.

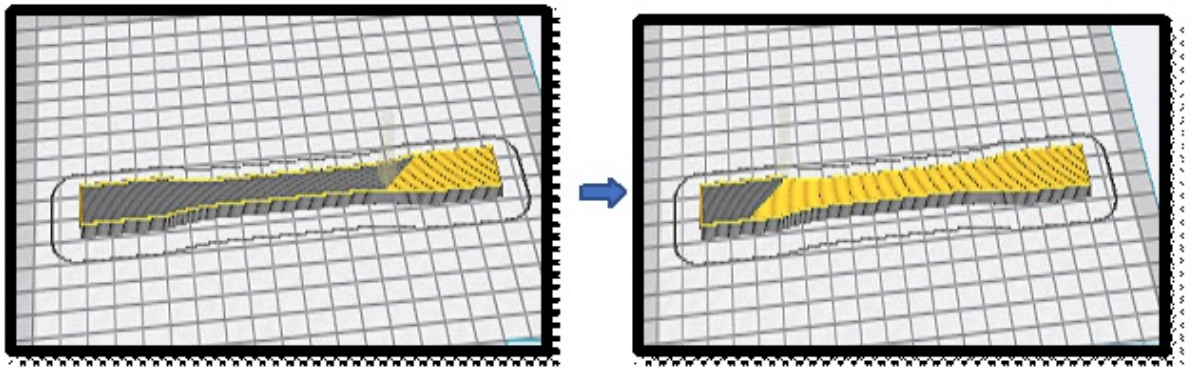

Figure 3.4: Tensile Specimen printing simulation.

The Tensile specimen printing in the 3D printer is shown in Figure 3.5. The part and scrap weight are weighed using a digital scale. The power consumption is measured using the Kill A Watt electricity usage monitor. Part weight, scrap weight, energy consumption, and printing time are all recorded during printing.

Figure 3.5: Tensile Specimen printing in 3D printer.

Table 3.1: Creality 3D printer specifications

Printer properties	Value
Build Volume	220 x 220 x 250 mm
Layer Resolution Low	0.4 mm
Layer Resolution High	0.1 mm
Nozzle Diameter	0.4 mm
Filament Diameter	1.75 mm

3.4 Printing Control Parameters and Settings

Examined 3D printing outcomes are the printing time, part weight, scrap weight, power consumption, and mechanical properties. The control parameters are the wall thickness, layer height, infill density, infill pattern, print speed, and print temperature. According to Taguchi's principles, the choice of OA depends on the overall degrees of freedom (DF) of the processing parameters and levels. Six processing parameters are identified. Five of these parameters have three levels with two DF, while one parameter has two levels with a single DF, resulting in a total of 11 DF. The DF is defined as the number of levels subtracted by one (DF = number of levels -1).

To achieve the best parameter configuration, the choice of OA must be equal to or greater than the total number of DF, as recommended by Taguchi. After evaluating several OA designs, the L18 OA is used for the experiment. The L18 OA has the smallest array with 17 Degrees of Freedom, allowing all six processing parameters to be adequately captured. Ranges of process parameters are used in determining levels for each parameter to find the optimal parameter combination. Thus, the relationship of the six parameters is determined at two to three levels. The samples printed with different infill densities and

infill patterns are shown in Figure 3.6. Table 3.2 lists factors and levels of the experimental design. The AM process parameters or control factors are explained as follows.

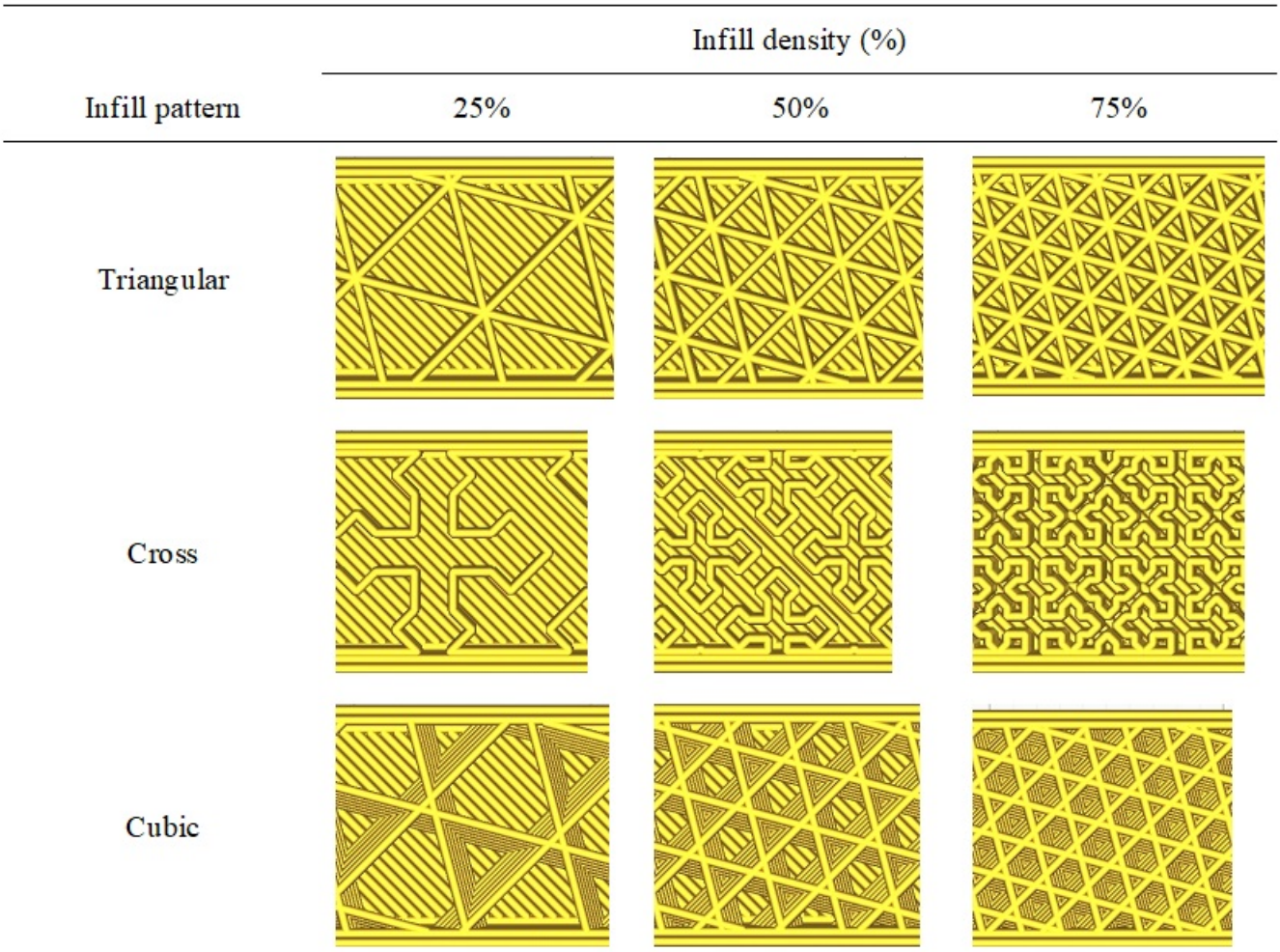

Figure 3.6: 3D printed samples.

3.4.1 Wall Thickness

The wall thickness is the horizontal thickness of the model's walls, decided by dividing the wall thickness by the wall line width for the number of walls. It is the minimum thickness of a 3D model. The structure of a 3D model has a significant impact on the minimum wall thickness. Figure 3.7 shows the wall thickness, infill pattern of a cross-sectional 3D

printed product. Two different levels of the wall thickness, 0.8 and 1mm, are considered in this research.

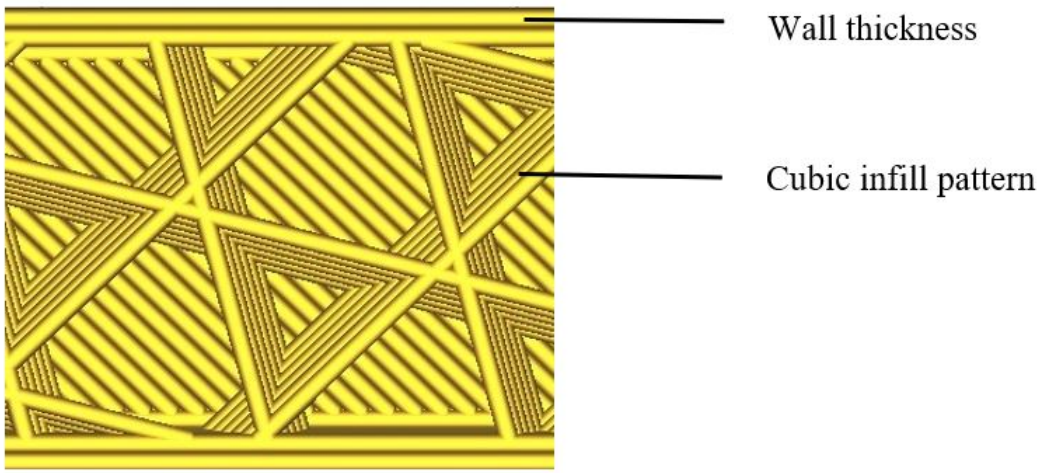

Figure 3.7: Different 3D printing parameters.

3.4.2 Layer Height

The layer height describes the height of each layer of material that a 3D printer extrudes, or sinters as shown in Figure 3.7. Layer height is one of the user-controlled parameters that can be changed using 3D printer software, although the minimum and maximum layer heights are constrained by the printer's physical features, such as the nozzle diameter. 0.1, 0.2, and 0.3mm layer heights are used in this research.

3.4.3 Infill Density

It is the amount of material used to fill the printing interior. Printing can be completed quickly if the low infill percentage is used. In this study, three infill percentage values 25%,50%, and 75% are used.

3.4.4 Infill Pattern

It is the inside framework of a 3D-printed component. Different shapes can be used to form this internal structure for the required structural integrity. Infill patterns affect the component weight, strength, and printing time. This research uses triangular, cross, and cubic infill pattern as shown in Figure 3.6.

3.4.5 Printing Speed

It is the movement rate of the printer head along X and Y axes to deposit layers of the material. Printing speeds of 50, 75, and $100mm/s$ are employed in this research.

3.4.6 Printing Temperature

It is the extrusion temperature of the 3D printer. The temperature affects the consistency and quantity of extruded filament in printing. Three different temperatures are considered in this research as shown in Table 3.2.

Table 3.2: Experimental parameters and levels.

Factor	Level 1	Level 2	Level 3
Wall thickness (mm)	0.8	1	-
Layer height (mm)	0.1	0.2	0.3
Infill density (%)	25	50	75
Infill pattern	Cubic	Triangular	Cross
Print speed (mm/s)	50	75	100
Printing temperature (℃)	200	210	220

3.5 Material Selection

Material selection for a 3D printer involves choosing the appropriate type of material to use as the raw substance for creating the printed objects. There is a range of materials available for 3D printing, including plastics (PLA, ABS), resins, metals, ceramics, and composite materials. Acrylonitrile Butadiene Styrene (ABS) and PLA are the two most used thermoplastic polymers utilized in FDM (Alhubail 2012). The choice depends on the specific application and desired properties of the final product such as strength, flexibility, and heat resistance. Some materials are better suited for prototyping, while others are designed for end-use products or specialized applications. Factors like cost, durability, ease of use, and environmental impact also influence material selection for 3D printing. Since PLA has excellent mechanical strength and affordability, we chose the PLA material for this study. The material filament is 1.75 mm in diameter with an accuracy of +/- 0.01 mm.

3.6 Experimental Design using the Taguchi Method

The Taguchi method is employed to analyze the effects of the process parameters on the response variables. It involves conducting a series of experiments to determine the settings of various factors or parameters that influence the output or performance of a system. The experiment searches for effects of control factors for the part characteristics. A mixed-element orthogonal array is a matrix with $m+n$ columns and N rows, where initial m columns contain s items and subsequent n columns contain t elements. This matrix is denoted by $OA_N(S^m \times t^n)$. A typical mixed-element array is $OA_N(2^1 \times s^m)$, where s is a prime integer (like 3 or 5) or a power of a prime number and $N = 2s^2$. OA_N $(2^1 \times s^m)$ represents a $N/(2^1 \times s^m) = (1/s)^{m-2}$ fractional factorial plan. Therefore, $OA_{18}(2^1 \times 3^5)$

is a part of a complete $(2^1 \times 3^5)$ factorial design, that is $(1/3)^{5-2} = (1/3)^3$ (Kacker et al. 1991).

There are two levels (1, 2) of the wall thickness and three levels (1, 2, 3) of the other five factors, where levels 1, 2, and 3 represent low, medium, and high levels of related factors. Therefore, the L18 orthogonal array $OA_N(S^m \times t^n)$ is formed based on factors and levels. The orthogonal design is written as $OA_{18}(2^1 \times 3^5)$, where $t = 2, n = 1, s = 3 and m = 5$. Number of columns for matrix= $m + n = 5 + 1 = 6$. The number of rows for matrix $N = 2s^2 = 18$.

Effects of processing factors on the response variables are assessed using the Taguchi L18 OA. For each combination of control factors and levels, experiments are conducted. Table 3.4 displays the L18 OA design with combinations of parameters used in the study. The data are statistically analyzed based on the Taguchi S/N ratio response (Huynh et al. 2017). The S/N ratio formula is shown in Table 3.3, where n represents the number of experiments performed, Y refers to the measured value and represents the standard deviation. The larger-better S/N ratio is employed for the ultimate tensile strength, tensile modulus, and compressive strength. The smaller-better S/N ratio is used for examining the printing time, energy use, and material use.

Table 3.3: Signal to noise (S/N) ratio (Huynh et al. 2017).

S/N ratio	Experimental objective	S/N ratio formula
The bigger, the better	Maximize the response	$\frac{S}{N} = -10log(\sum \frac{\frac{1}{Y^2}}{n})$
The smaller, the better	Minimize the response	$\frac{S}{N} = -10log(\sum \frac{Y^2}{n})$
Closer to the nominal value, the better	Nominal is the target	$\frac{S}{N} = -10log(\sigma^2)$

Table 3.4: L18 orthogonal array design.

Sample	Wall thickness	Layer height(mm)	Infill density (%)	Infill pattern	Print speed	Printing temperature ($°C$)
1	0.8	0.1	25	Cubic	50	200
2	0.8	0.1	50	Triangular	75	210
3	0.8	0.1	75	Cross	100	220
4	0.8	0.2	25	Cubic	75	210
5	0.8	0.2	50	Triangular	100	220
6	0.8	0.2	75	Cross	50	200
7	0.8	0.3	25	Triangular	50	220
8	0.8	0.3	50	Cross	75	200
9	0.8	0.3	75	Cubic	100	210
10	1	0.1	25	Cross	100	210
11	1	0.1	50	Cubic	50	220
12	1	0.1	75	Triangular	75	200
13	1	0.2	25	Triangular	100	200
14	1	0.2	50	Cross	50	210
15	1	0.2	75	Cubic	75	220
16	1	0.3	25	Cross	75	220
17	1	0.3	50	Cubic	100	200
18	1	0.3	75	Triangular	50	210

3.7 Analysis of Variance (ANOVA)

The analysis of variance (ANOVA) technique is typically used to examine process factors on quality attributes. The importance of the predictor on responses is assessed using the F-statistic and p-values of the ANOVA result (Gregorian et al. 2001). ANOVA is used to identify the key process variables for influencing the overall objective, evaluate experiment data, and draw conclusions.

ANOVA is employed in this research to evaluate comparison experiments for the single difference in significance. The statistical significance of the experiment is determined

by the ratio of the two variances, and this ratio remains consistent even when certain alterations are made to the experimental findings. It remain unaffected by the addition of a constant to all observations, and similarly, the significance doesn't change when all observations are multiplied by a constant. Using ANOVA, the equation for sample variances is as follows in Equation 3.1 (Wiki 2023a).

$$S^2 = \frac{1}{N}\sum_{i=1}(y_i - \bar{y})^2 \tag{3.1}$$

where the squared terms represent deviations from the sample mean, the divisor (N) is referred to as degrees of freedom (DF), and the sum is the sum of squares (SS). The result is the mean square (MS). There are three sample variances: a total variance based on all observational departures from the mean, an error variance based on all observational deviations from the means of the applicable treatments, and a treatment variance (Standard 2012). To consider the discrepancy between the variance of observations and variance of means, the treatment variance is based on departures of treatment means from the overall mean. The primary procedure includes dividing the entire sum of squares (SS) into parts that are connected to the model effects as shown in Equation 3.2.

$$SS_{Total} = SS_{Error} + SS_{Treatments} \tag{3.2}$$

where sum of squares (SS) is used to determine the number of DF, the component for error, provides a Chi-squared distribution that defines the sum of squares associated with it, but the component for "treatments" specifies the same thing if there is no treatment effect. A general equation for degree of freedom (DF) is shown in Equation 3.3.

$$DF_{Total} = DF_{Error} + DF_{Treatments} \tag{3.3}$$

The p-value is a statistical measure used in Analysis of Variance (ANOVA) to assess the significance of group mean differences or the impact of a factor on observed variability

between groups. Because these analytical techniques are based on their hypothesis testing on probability or P-value, the lower the P-value, the greater the likelihood that the null hypothesis will be rejected. As a result, the parameter or interaction is regarded as significant (Huang et al. 2018). For comparing components of the overall deviation, the F-test is employed. The F-value in an ANOVA is determined by dividing the variation in sample means by the variation in the samples, as shown in Equation 3.4. For instance, in one-way or single-factor ANOVA, the F-test statistic is used to compare the statistical significance (Rouf et al. 2022).

$$F = \frac{\text{Variance between treatments}}{\text{Variance within treatments}} \tag{3.4}$$

In terms of minimizing false negative errors for a fixed rate of false positive errors, the ANOVA F-test is used. ANOVA applies to the investigation of the combined effects of several variables. Factorial experiments are those that include observations across all possible values of each factor. Factorial experiments are more effective than a series of experiments with a single factor. The effectiveness increases with the number of factors (Qattawi et al. 2017).

The term "adjusted R-squared" refers to a version of R-squared that is changed to account for the number of predictors in the model. A corrected model accuracy indicator for linear models is called an adjusted R-square. When the additional term enhances the model more than that anticipated by chance, the adjusted R-squared rises. It falls off when a predictor makes a smaller contribution to model improvement than the anticipated value. A normal adjusted R-squared value is one that is positive. It is always less than the R-squared value (Upcraft and Fletcher 2003).

3.8 Measurement and Testing Methods

3.8.1 Measurement of Part Weight and Scrap Weight

The material consumption includes the main part and scrap in weight. The part weight corresponds to the material used to build the part, whereas the scrap weight corresponds to the support material used during printing. Figures 3.8 and 3.9 show the part weight measurement and scrap weight measurement. Weights of both parts and scrap are measured using a digital laboratory scale.

Figure 3.8: Part weight measurement.

3.8.2 Measurement of Printing Time

The measurement of printing time for a 3D printer involves determining the total time required for the printer to complete the fabrication of the specific object or model. This includes every step of the procedure, from the start of printing to the end of the last layer. Accurate printing time measurement is essential for 3D printing processes that maximize productivity and resource usage. The printing time is collected for the 18 samples during printing for further analysis to find out the time used for different combinations of parameter settings.

Figure 3.9: Scrap weight measurement.

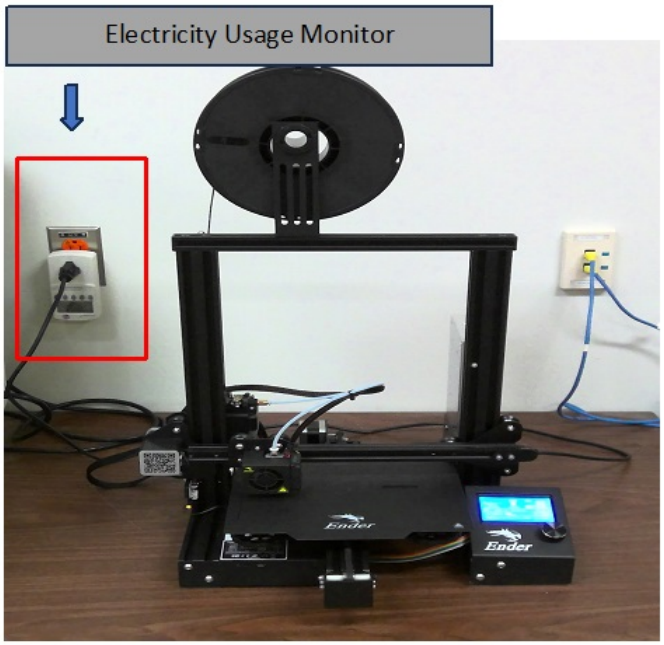

Figure 3.10: Measurement of the power consumption.

3.8.3 Measurement of Power Consumption

Power consumption data are collected using a P4400 Kill A Watt Electricity Usage Monitor, which quantifies energy usage in kilowatt-hours (kWh). To capture power consumption

metrics, the 3D printer is connected to this electricity usage monitor and securely plugged into a socket, as depicted in Figure 3.10. Table 3.5 represents the calculative power consumed by 3D printed parts. The following power formula is used to calculate the power consumption in Equation 3.5.

$$\text{Power consumption} = \text{Power (kW)} \times \text{Production Time (h)} \tag{3.5}$$

Table 3.5: Power consumption data for tensile testing samples

Specimen	Production time (h)	Power(KW)	Power consumption (h KW)
L1R	1:17:00	0.11KWH	0.13
L2R	1:10:43	0.10KWH	0.11
L3R	2:10:24	0.20KWH	0.42
L4R	0:39:39	0.05KWH	0.02
L5R	0:38:50	0.06KWH	0.02
L6R	1:20:17	0.11KWH	0.13
L7R	0:45:00	0.06KWH	0.03
L8R	0:41:21	0.06KWH	0.02
L9R	0:33:19	0.05KWH	0.02
L10R	1:05:03	0.09KWH	0.09
L11R	1:29:34	0.13KWH	0.17
L12R	1:21:07	0.11KWH	0.13
L13R	0:34:55	0.05KWH	0.02
L14R	1:06:49	0.09KWH	0.1
L15R	0:47:25	0.07KWH	0.03
L16R	0:37:16	0.05KWH	0.02
L17R	0:32:11	0.04KWH	0.01
L18R	0:49:00	0.07KWH	0.03

3.8.4 Tensile Testing

Tensile testing examines two key parameters: tensile strength and tensile modulus. By examining stress/strain curves relevant to the composite polymers, they can be calculated. The ability of a material to resist being pulled apart is measured by its tensile strength.

Tensile stress is defined using Equation 3.6:

$$\sigma = \frac{F}{A} \tag{3.6}$$

where, σ is tensile stress in megapascals (MPa), F is the measured force associated in Newton, and A is the initial cross-sectional area of the specimen in square millimeters.

If yielding occurs before or at the point of tensile strength, the tensile strain at the moment is given as a dimensionless ratio or in percentage (%). The starting distance between the grips is used to calculate the strain, defined in Equation 3.7.

$$\epsilon = \frac{\Delta L}{L} \tag{3.7}$$

where, ϵ is the tensile strain, expressed as a dimensionless ratio or percentage, L is the gauge length of the test specimen, expressed in millimeters, and ΔL is the increased distance in the specimen length between the gauge marks, expressed in millimeters. The sample tensile is tested using an MTS universal testing machine. The specimen's two grips are used to secure it in the tensile testing equipment. The crosshead speed applied is 1 mm/min in room temperature. Tensile stress is tested using stretching or tensile forces.

The material elongates along the axis of the applied load as shown in Figure 3.11. Megapascals (MPa) is the unit of measurement, and all stress values are determined using the specimen's original cross-sectional area. Figure 3.12 shows fractured samples after the tensile test elongation.

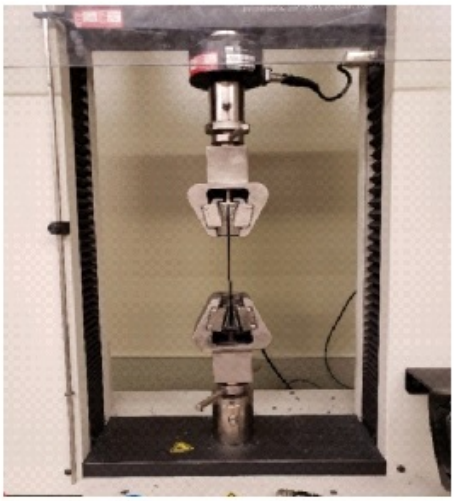

Figure 3.11: MTS universal testing machine.

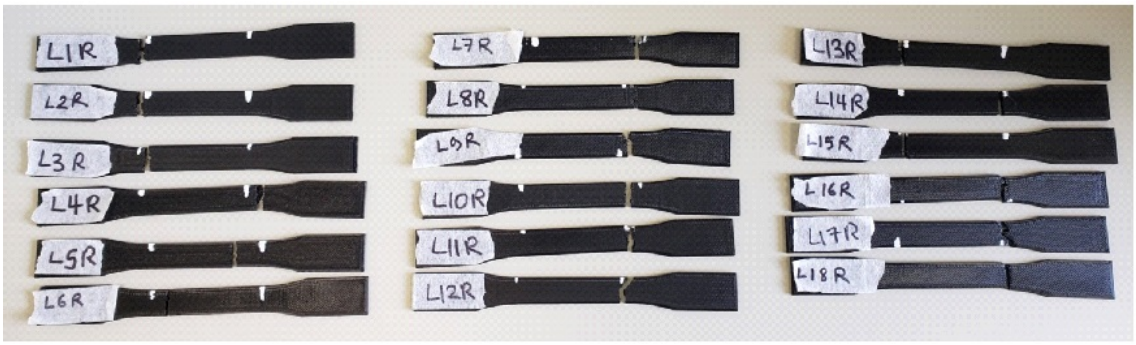

Figure 3.12: Fractured tensile samples.

3.8.5 Compression Testing

Total 18 specimens are manufactured using the FDM method to analyze the mechanical strength properties. Values for compressive stress (in MPa) are determined through compression tests. A universal Instron testing machine is used for compression testing. The specimens are compressed by 9.88 mm along with 50% strain as shown in Figure 3.13 (i). During the test, a preload of 100 kN and a speed of 5 mm/min are applied. The compressive stress is computed based on the experimental results. Figure 3.13 (ii) shows the compressed sample after the compression. The test data are

collected during the experiment.

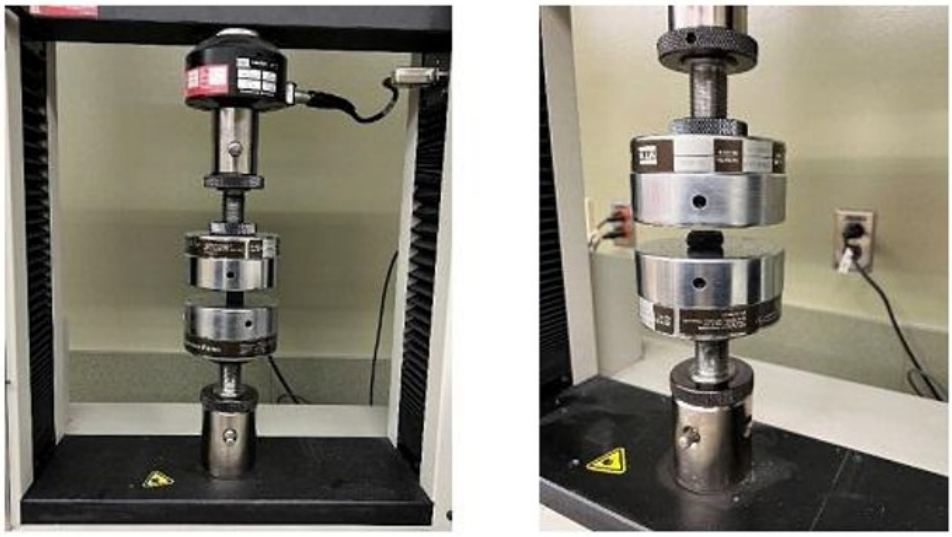

i. ii.

Figure 3.13: Compression testing procedures (i) Sample before compression and (ii) Sample after compression.

In summary, this chapter outlines methods for performing experiments, including the choice of variables, creation of specimens, and simulation of printing samples. The chapter also provides a thorough description of the 3D printer used for its features and technical details. In addition, it describes the control parameters and settings used in printing. Furthermore, the material selection criteria are also discussed. Methods of the measurement and testing are explained for the data analysis.

Chapter 4

Experimental Results and Discussion

4.1 Experimental Data Collection

Parameter settings are investigated using the data obtained in the 3D printing process along with tensile and compression tests. The printing time, part weight, scrap weight, and power consumption are to be minimized while the tensile modulus, ultimate strength, and compressive stress are to be maximized. According to the orthogonal design, 18 specimens for the tensile and compression tests are printed using an FDM printer, and tensile and compression experiments are carried out to gather the necessary data. The collected data are shown in Table 4.1.

4.2 Data Analysis

The collected data are analyzed using Minitab-19 statistical software. Means and S/N ratios are used to determine the ideal combination of parameters. To find the contributions of each control parameter to the response variables, the ANOVA analysis is used to evaluate the data for conclusions. Optimization of the response variables is searched in the Desirability Function Analysis (DFA).

Table 4.1: Experimental data collected.

Specimen	Power consumption	Scrap Weight	Part Weight	Printing time	Compressive stress	Ultimate tensile strength	Tensile modulus
	(KWH)	(g)	(g)	(min)	(Mpa)	(MPa)	(MPa)
L1R	0.11	0.1	5.22	77	28.4	16.5	501.53
L2R	0.1	0.15	6.67	70	43	18.5	615.63
L3R	0.2	0.15	7.4	130	65.8	15.9	555.83
L4R	0.05	0.17	6.49	39	13.3	22.15	670.56
L5R	0.06	0.08	7.48	38	29.6	24.43	719.33
L6R	0.11	0.17	7.8	80	65.7	18.9	628.62
L7R	0.06	0.2	7.9	45	15.9	27.4	512.74
L8R	0.06	0.11	8.07	41	29.7	25.52	782.53
L9R	0.05	0.13	8.84	33	62.6	30.2	829.93
L10R	0.09	0.14	5.24	65	30.1	14.9	438.39
L11R	0.13	0.12	6.7	89	42.1	21.6	633.09
L12R	0.11	0.11	7.7	81	58.9	20.55	661.57
L13R	0.05	0.11	6.36	34	14.9	21.13	585.52
L14R	0.09	0.07	7.13	66	40.1	19.7	612.63
L15R	0.07	0.12	8.4	47	75.8	31.12	830.65
L16R	0.05	0.14	7.84	37	15.2	29.6	787.32
L17R	0.04	0.11	8.1	32	27.7	25.4	710.39
L18R	0.07	0.07	8.87	49	61.1	32.9	920.67

4.3 Material Consumption

To analyze the material consumption of the printed part, weights of the sample's part and scrap material are measured and recorded as shown in Table 4.1. Figure 4.1 displays the part weight of the samples. It is noticed that samples 1 and 10 have the lightest part

weight, followed by samples 4 and 13. All these samples have an infill density of 25%.

Figure 4.1: Part Weight.

Sample 1 is lighter than sample 10 by 0.02g. These two samples have the same density and layer height. They differ in the wall thickness, infill pattern, print speed, and print temperature. The thicker wall of sample 10 could explain the heavier weight. However, comparing samples 1 and 4, the latter is heavier while having the same wall thickness, infill density, and infill pattern. The taller layer height of sample 4 contributes to a heavier sample. However, comparing samples 4 and 13, the latter is lighter while having the same layer height and thicker wall because sample 13's triangular infill pattern makes it lighter than sample 4's cubic pattern. However, comparing samples 4 and 7, the former is much lighter while having a cubic pattern as opposed to sample 7's triangular pattern.

Looking at the printing temperature and speed, sample 10 is higher and faster than sample 1 in slightly heavier. Having a high printing temperature and low printing speed means more filaments come out, while having a high temperature and speed means less filament comes out. Sample 10 has a thicker wall, but less filament is being extruded,

making it only slightly heavier than sample 1, which has a thinner wall but more filament extrusion. Sample 4 is heavier as its printing speed is slower and temperature is higher than sample 13. As a result, sample 13 is lighter than sample 4.

A combination of fast printing speed and high print temperature means more filament is being extruded. The combination of a fast printing speed and low printing temperature means less filament is being extruded. Additionally, the combination of a slow printing speed and high printing temperature means the most filament is being extruded. Lastly, a slow printing speed and low temperature mean more filament is being extruded.

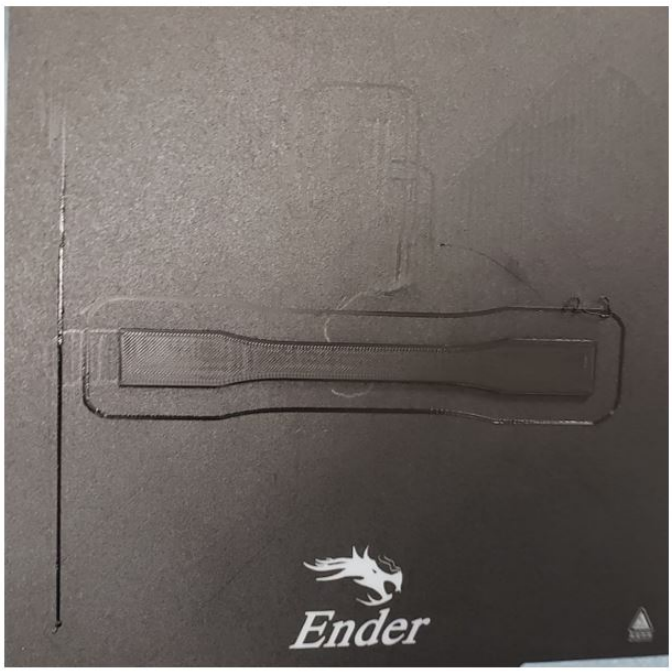

Figure 4.2: Printing bed.

Figure 4.2 is the printing bed with a printed sample. On the right side of the printing bed, there is the initial calibration of the 3D printer before printing. Around the sample is the skirt to help prepare the extruder. Pulling these off the printing bed is difficult and inconsistent as some pieces would get stuck on the bed. As a result, the scrap weight is collected carefully.

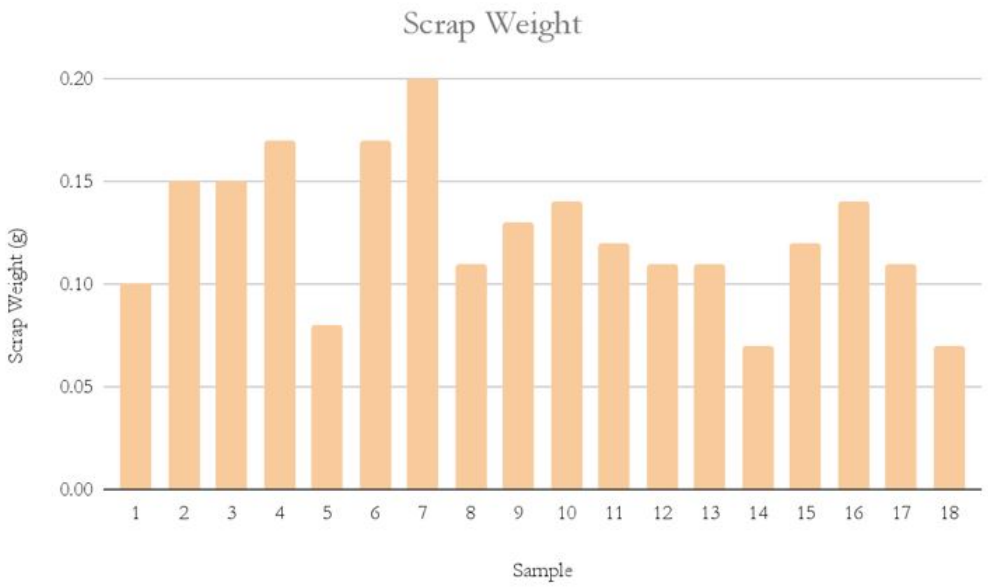

Figure 4.3: Scrap weight.

Orthogonal arrays are designed using the DOE method for the experimental trials. The signal-to-noise (S/N) ratio graph is used to minimize process variability and evaluate effects of parameter interactions. The main effect plots are generated. Effect plots for the part weight and scrap weight are displayed in Figures 4.4 (a) and (b), respectively. The least layer height value, cross infill pattern, and least infill density can reduce the material use. In comparison to other factors, the wall thickness has the least impact on the part weight.

Table 4.7 shows the S/N response for the part weight, and it shows the delta value and rank for parameters to understand the parameter effects on the response. The difference between the greatest and minimum average response (standard deviation or signal-to-noise ratio) for the factor is known as the delta. Each Delta is given a rating, with Rank 1 designating the largest Delta (Ryan 2023). It can be concluded that A1B1C1D3E3F2 is the optimal parameter combination for the lowest part weight. The optimum combination of parameters is given by wall thickness at level 1, which is 0.8 mm, layer height of 0.1

mm at level 1, infill density of 25% (level 1), infill pattern at level 3, which is a cross infill pattern, printing speed at 100 mm/s (level 3), and printing temperature of 210 °C at level 2. The parameters with levels are shown in Table 4.2.

Table 4.2: Parameters and levels.

Factor	Level 1 (High)	Level 2 (Medium)	Level 3 (Low)
Wall thickness (A)	0.8	1	-
Layer height (B)	0.1	0.2	0.3
Infill density (C)	25	50	75
Infill pattern (D)	Cubic	Triangular	Cross
Print speed (E)	50	75	100
Printing temperature (F)	200	210	220

4.4 Time Consumption

According to the main effects plot for printing time in Figure 4.6 (a). The specimen shows the least printing time when using the 25% infill density, 100 mm/s printing speed, maximum layer height, and cubic filling pattern. Based on S/N ratio in Table 4.3, when the layer height increases, fewer layers are required to construct the item, and the number of layers is reduced to reduce the processing time. S/N ratio, which indicates whether the noise level is affecting the desired signal, can be calculated using a predefined formula that compares the two levels and yields the ratio. Usually, a single decibel (dB) value is used to indicate the ratio. The ratio may have three possible values: zero, positive, or negative. A negative signal-to-noise ratio (SNR) indicates a lower signal power than

noise. The combination of A2B3C1D1E3F2 gives in the least printing time.

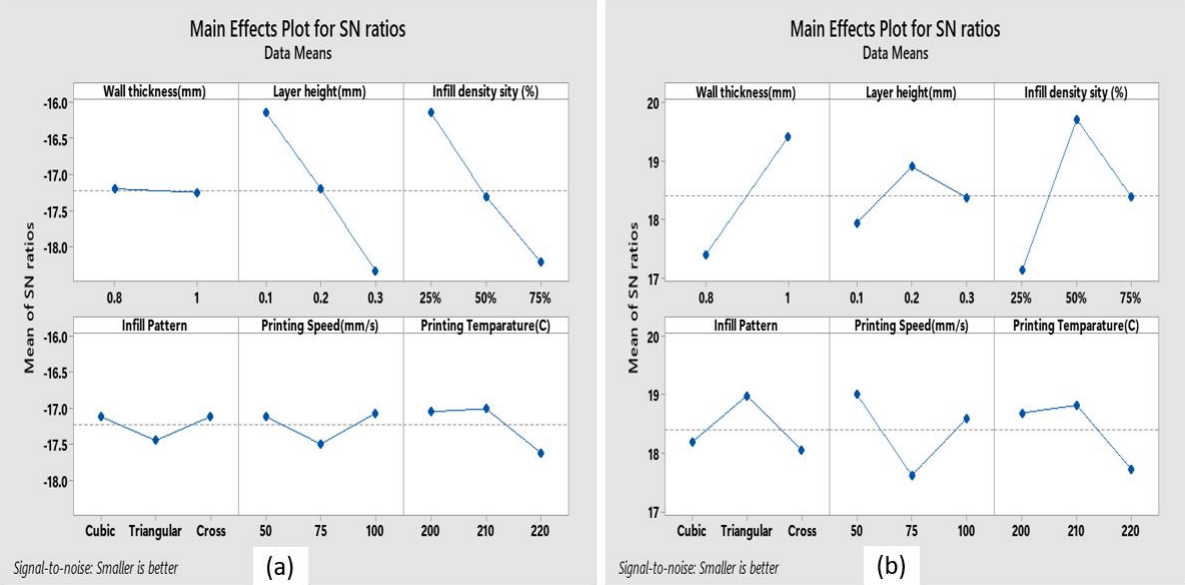

Figure 4.4: Main effect plot for S/N ratio. (a) Part weight, (b) Scrap weight.

4.5 Power Consumption

The power consumption for various samples is shown in Figure 4.5. Samples with the shortest printing time consume the least amount of power. These samples are 4, 5, 7, 8, 9, 13, 16, and 17. Parameters that greatly affect printing time and power consumption are the layer height and printing speed. It is noted that sample 17 consumes the least amount of power.

The power used shows a similar pattern to the printing time in Figure 4.6 (b). The layer height and printing speed have significant effects on power usage. The best combination of parameters shown in Table 4.6 is A2B3C1D1E3F1. Power consumption is reduced along with the reduction of processing time.

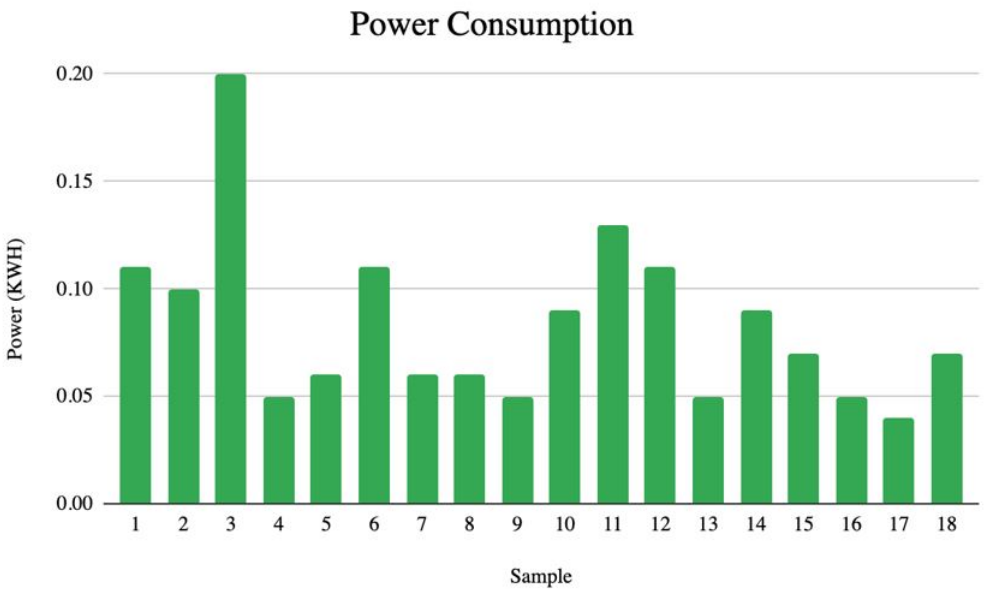

Figure 4.5: Power Consumption.

Table 4.3: S/N response for printing time.

Level	Wall thickness	Layer height	Infill density	Infill Pattern	Printing Speed	Printing temperature
1	-34.9	-38.4	-33.48	-33.74	-36.34	-34.49
2	-34.35	-33.7	-34.37	-34.03	-33.99	-34.26
3		-31.8	-36.02	-36.1	-33.54	-35.12
Delta	0.55	6.56	2.54	2.36	2.8	0.86
Rank	6	1	3	4	2	5

4.6 Mechanical Properties of Samples

4.6.1 Tensile Properties

Main effects plots of the ultimate tensile strength (UTS) and tensile modulus for specimens are shown in Figures 4.7 (a) and (b) to determine the optimal set of parameters for the greatest tensile strength. Figure 4.7 (a) shows that if we increase the wall thickness, layer

height, infill density, and printing temperature, and reduce printing speed using a cubic infill pattern, the UTS can be improved.

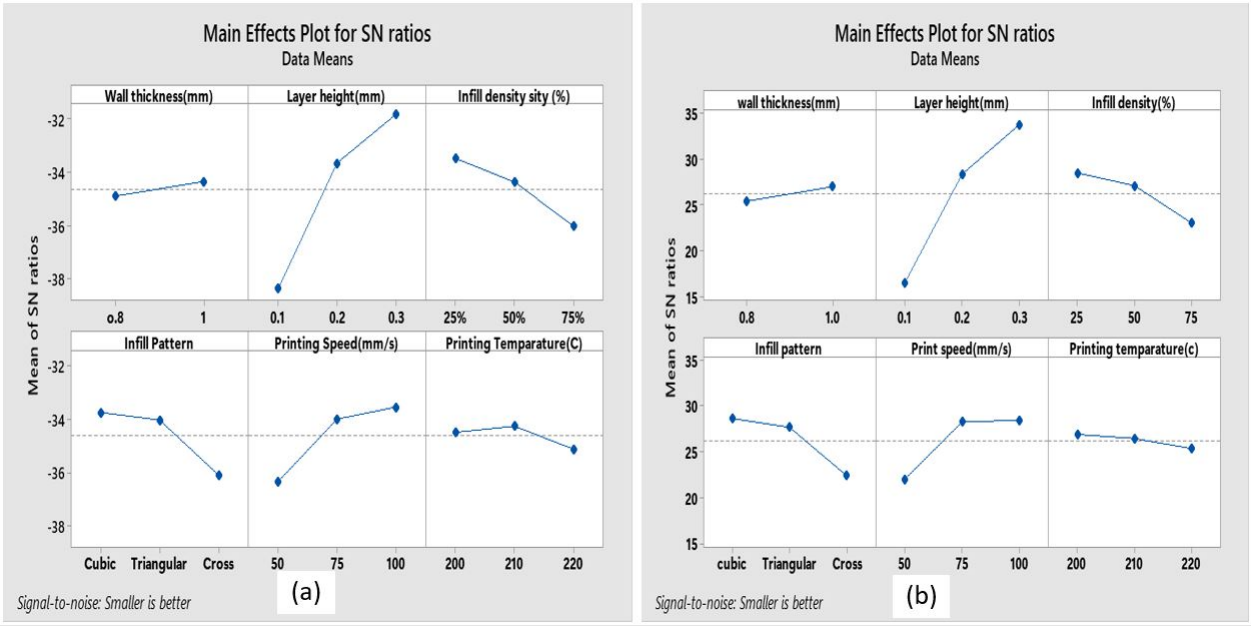

Figure 4.6: S/N ratio effect plots. (a) Printing time, (b) Power consumption.

The ideal parameter combination determined by the S/N ratio analysis is shown in Tables 4.4 and 4.5 for UTS and tensile modulus, respectively. The findings demonstrate that the layer height has the biggest impact on both tensile strength and tensile modulus. It can be concluded that the combination of parameters with wall thickness at 1 mm, layer height of 0.3 mm, infill density of 50%, infill pattern of triangular, printing speed at 75 mm/s and printing temperature at 220, or A2B3C3D1E2F3, gives the maximum tensile strength. Similarly, based on the S/N ratio in Figure 4.7 (b), it can be concluded that the combination of A2B3C3D1E2F2, i.e., wall thickness of 1 mm, layer height at 0.3, infill density of 75%, infill pattern for cubic, printing speed of 75mm/s and printing temperature of 210℃, gives the optimal tensile modulus.

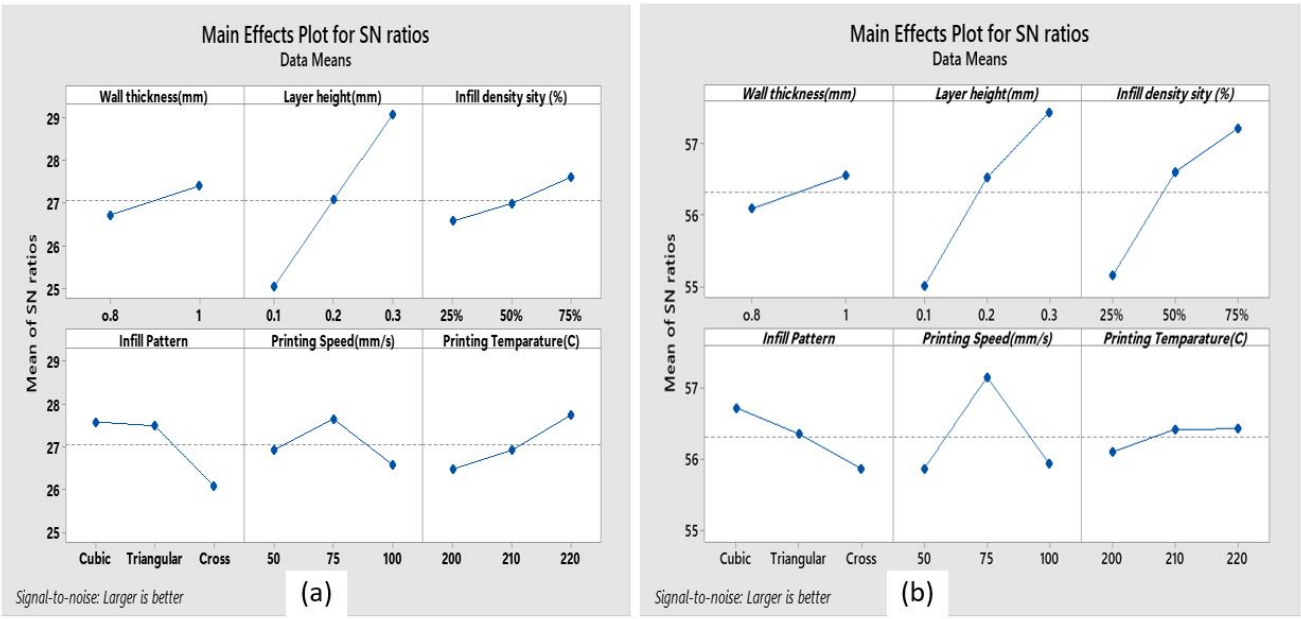

Figure 4.7: S/N ratio effect plots. (a) Ultimate tensile strength (UTS), (b) Tensile modulus.

Table 4.4: S/N response table for the UTS.

Level	Wall thickness	Layer height	Infill density	Infill Pattern	Printing Speed	Printing temperature
1	26.71	25.02	26.57	27.58	26.93	26.48
2	27.39	27.07	26.99	27.49	27.65	26.92
3		29.06	27.6	26.08	26.57	27.75
Delta	0.68	4.04	1.04	1.5	1.08	1.27
Rank	6	1	5	2	4	3

4.6.2 Compressive properties

Based on data in Table 4.8, the infill density has the biggest impact on the compressive stress. The layer height and printing speed also impacts the compressive stress. Figure 4.9 shows the compressive stress vs strain curve for samples from the compression test.

Table 4.5: S/N response table for the UTS.

Level	Wall thickness	Layer height	Infill density	Infill Pattern	Printing Speed	Printing temperature
1	56.09	54.99	55.14	56.73	55.87	56.11
2	56.56	56.52	56.6	56.36	57.15	56.44
3		57.45	57.22	55.87	55.94	56.43
Delta	0.47	2.45	2.08	0.85	1.28	0.32
Rank	5	1	2	4	3	6

The samples are labeled in the graph such as Sample 1 represents L1, Sample 2 for L2. The highest peak compressive stress is achieved by sample 15 with 75.8 MPa. Sample 4 has the lowest peak compressive stress 13.3 MPa among all samples. It is evident that each run produces distinct results based on the settings for the parameter combinations used in the factorial design. At a high level of the wall thickness, better compressive stress is produced by the 75% infill density for the samples. Values in the compression tests support this situation. The best combinations of the suggested parameters are identified by the DOE approach. Outcomes of this investigation show that the impact of layer height varies for each output. The wall thickness in 1 mm, cubic, and cross structures often produces the best result when the infill density is 75%. The infill density varies depending on the infill pattern.

Effects graphs for the means and S/N ratio analyses are shown in Figure 4.8. The combination of A2B1C3D3E1F2, i.e., 0.8mm of wall thickness, 0.1mm layer height, infill density of 75%, cross infill pattern, 50mm/s printing speed , and 210℃ printing temperature , achieves the ideal compression performance.

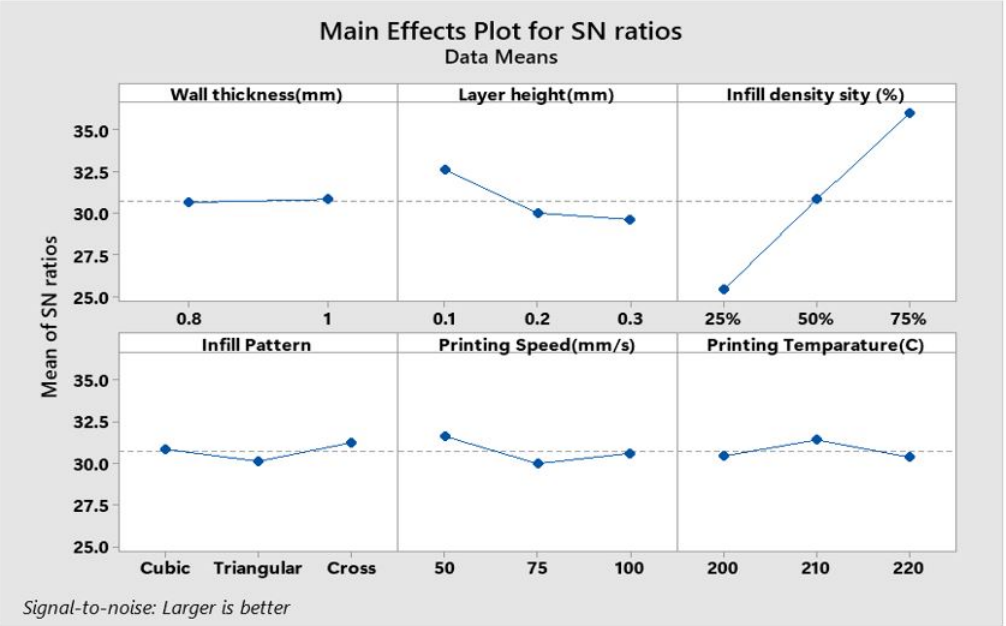

Figure 4.8: Effect plots S/N ratio for compressive stress.

Table 4.6: S/N response for energy consumption.

Level	Wall thickness	Layer height	Infill density	Infill Pattern	Printing Speed	Printing temperature
1	25.39	16.41	28.51	28.59	21.96	26.85
2	26.99	28.35	27.09	27.63	28.21	26.42
3		33.81	22.98	22.36	28.4	25.3
Delta	1.6	17.4	5.53	6.23	6.44	1.55
Rank	5	1	4	3	2	6

4.7 ANOVA Statistical Analysis

ANOVA is used to further determine the effects of control factors on the process response. An F-test and the analysis of variance is used to determine the impact of each component. These analyses use a 95% confidence level.

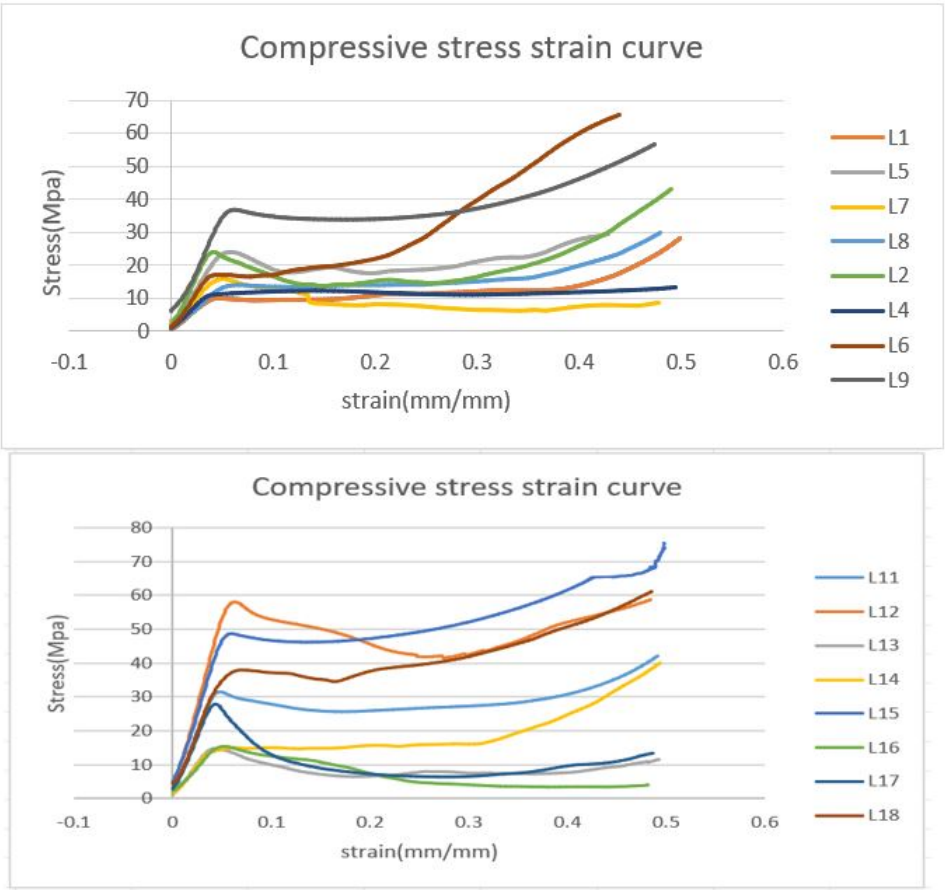

Figure 4.9: Stress-Strain graph for compression testing samples.

Table 4.7: S/N response for the part weight.

Level	Wall thickness	Layer height	Infill density	Infill Pattern	Printing Speed	Printing temperature
1	-17.2	-16.14	-16.15	-17.12	-17.11	-17.05
2	-17.25	-17.2	-17.31	-17.45	-17.49	-17.01
3		-18.34	-18.22	-17.11	-17.07	-17.62
Delta	0.05	2.2	2.07	0.33	0.42	0.61
Rank	6	1	2	5	4	3

The proportion of contributions in ANOVA is employed for the effect analysis because the Taguchi approach could not determine the impact of individual parameters on the

Table 4.8: S/N response for compressive stress.

Level	Wall thickness	Layer height	Infill density	Infill Pattern	Printing Speed	Printing temperature
1	30.64	32.59	25.37	30.84	31.62	30.43
2	30.82	30	30.82	30.12	29.98	31.41
3		29.6	36	31.24	30.6	30.36
Delta	0.18	2.99	10.63	1.12	1.64	1.04
Rank	6	2	1	4	3	5

total process. The proportion of factor contributions to the total shows the effect of reducing variation. A modest change will have a significant impact on performance when a factor makes up a high percentage of the contribution (Yang 2022). The percentage of contribution (f_i) is a function of the sum of squares for each item, is defined in Equation 4.1 as follows (Alhubail 2012).

$$f_i = \frac{SS'_{f_i}}{Seq\ SS_{TOTAL}} \tag{4.1}$$

where f_i is the ith factor, $SS'f_i$is the pure sum of squares for f_i, and $SeqSS_{TOTAL}$ is the mean of the sequential sum of squares overall. After analyzing the F value and percentage of contributions of printing parameters, the layer height shows the biggest impact on the mechanical strength (both for UTS and tensile modulus), where the infill density and layer height have the most impact on the compressive stress. The wall thickness has the least impact on all the response variables. The analysis of variance along with the contribution percentages has been conducted to find each parameter's contributions on the variables shown in Tables 4.9 to 4.14, where, DF represents degree of freedom between groups, Seq SS stands for Sequential Sum of Squares, which represents how each group or component contributes to the overall variability in the data with the use of the sequential sum of squares. The P value is used to determine the statistical significance of

the observed results.

Table 4.9: ANOVA and analysis of S/N ratio for UTS vs control parameters.

Source Contribution	DF	Seq SS	Adj SS	Adj MS	F	P	Contribution
Wall thickness(mm)	1	2.079	2.079	2.0794	6.08	0.049	2.82%
Layer height (mm)	2	48.925	48.925	24.463	71.54	0	66.54%
Infill density (%)	2	3.264	3.264	1.6319	4.77	0.057	4.44%
Infill Pattern	2	8.540	8.540	4.270	12.49	0.007	11.61%
Print speed (mm/s)	2	3.648	3.648	1.8238	5.33	0.047	4.96%
Printing (°C)	2	5.020	5.020	2.5102	7.34	0.024	6.83%
Residual Error	6	2.052	2.052	0.3419			2.79%
Total	17	73.528					100%

S=0.5847, R-Sq=97.21%, R-Sq(adj)=92.09%

Table 4.10: Analysis of S/N ratio for tensile modulus vs control parameters.

Source Contribution	DF	Seq SS	Adj SS	Adj MS	F	P	Contribution
Wall thickness(mm)	1	0.9899	0.9899	0.9899	0.81	0.403	2.009%
Layer height(mm)	2	18.401	18.4006	9.2003	7.51	0.023	37.35%
Infill density(%)	2	13.692	13.6919	6.8459	5.59	0.043	27.78%
Infill pattern	2	2.2013	2.2013	1.1007	0.9	0.456	4.47%
Print speed(mm/s)	2	6.2251	6.2251	3.1125	2.54	0.159	12.63/%
Printing (°C)	2	0.4145	0.4145	0.2073	0.17	0.848	0.84/%
Residual Error	6	7.3467	7.3467	1.2244			14.91/%
Total	17	49.27					100%

S=1.1065, R-Sq=85.09%, R-Sq(adj)=57.75%

4.8 Method Evaluation

The proposed method is evaluated by comparing the DOE method and lab testing solution for the prediction accuracy of the mechanical and sustainable characteristics of sample parts as shown in Table 4.15.

Table 4.11: Analysis of S/N ratio for energy consumption vs control parameters.

Source Contribution	DF	Seq SS	Adj SS	Adj MS	F	P	Contribution
Wall thickness(mm)	1	0.005	0.0050	0.0050	1.06	0.343	3.04%
Layer height(mm)	2	0.0786	0.0786	0.0393	8.35	0.018	47.26%
Infill density (%)	2	0.0181	0.0181	0.0091	1.92	0.227	10.88%
Infill pattern	2	0.0197	0.0197	0.0099	2.09	0.204	11.86%
Print speed(mm/s)	2	0.0072	0.0072	0.0036	0.77	0.505	4.34%
Printing (°C)	2	0.0094	0.0094	0.0047	1	0.422	5.67%
Residual Error	6	0.0282	0.0282	0.0047			16.99%
Total	17	0.1664					100%

S=0.686, R-Sq=83.01%, R-Sq(adj)= 51.87%

Table 4.12: ANOVA and contribution analysis for S/N ratio for printing time vs control parameters.

Source Contribution	DF	Seq SS	Adj SS	Adj MS	F	P	Contribution
Wall thickness(mm)	1	1.351	1.351	1.351	1.22	0.311	0.63%
Layer height(mm)	2	137.55	137.55	68.775	62.27	0	64.00%
Infill density (%)	2	19.972	19.972	9.986	9.04	0.015	9.29%
Infill Pattern	2	19.898	19.898	9.949	9.01	0.016	9.25%
Printing Speed(mm/s)	2	27.116	27.116	13.558	12.28	0.008	12.61%
Printing (°C)	2	2.399	2.399	1.199	1.09	0.396	1.11%
Residual Error	6	6.627	6.627	1.104			3.08%
Total	17	214.912					100%

S=1.0509, R-Sq=96.92%, R-Sq(adj)= 91.26%

The biggest disparity between the experimental and Taguchi method solutions is 9.24%. Therefore, it is concluded that the Taguchi approach can accurately predict the mechanical and other characteristics for 3D printed parts.

Table 4.13: ANOVA and contribution analysis for S/N ratio for part weight vs control parameters.

Source Contribution	DF	Seq SS	Adj SS	Adj MS	F	P	Contribution
Wall thickness(mm)	1	0.0120	0.0120	0.01199	0.11	0.756	0.39%
Layer height(mm)	2	14.473	14.473	7.23648	63.74	0	47.31%
Infill density (%)	2	12.9497	12.950	6.47486	57.03	0	42.33%
Infill Pattern	2	0.4308	0.4308	0.21541	1.9	0.23	1.41%
Printing Speed(mm/s)	2	0.6532	0.6532	0.32662	2.88	0.133	2.14%
Printing (°C)	2	1.3863	1.3863	0.69315	6.11	0.036	4.53%
Residual Error	6	0.6812	0.6812	0.11353			2.22%
Total	17	30.5862					100%

S=0.3369, R-Sq=97.77%, R-Sq(adj)=93.69%

Table 4.14: ANOVA contribution analysis of S/N ratio for compressive stress vs control parameters.

Source Contribution	DF	Seq SS	Adj SS	Adj MS	F	P	Contribution
Wall thickness(mm)	1	0.152	0.152	0.152	0.06	0.821	0.04%
Layer height(mm)	2	31.622	31.622	15.811	5.81	0.04	7.84%
Infill density (%)	2	338.84	338.84	169.42	62.2	0	84.05%
Infill Pattern	2	3.88	3.88	1.94	0.71	0.528	0.96%
Printing Speed(mm/s)	2	8.23	8.23	4.115	1.51	0.294	2.04%
Printing (°C)	2	4.085	4.085	2.042	0.75	0.512	1.01%
Residual Error	6	16.331	16.331	2.722			4.05%
Total	17	403.14					100%

S=1.6498, R-Sq=95.95%, R-Sq(adj)=88.52%

4.9 Desirability Function Analysis

Desirability Function Analysis(DFA) is used to optimize and evaluate multiple responses or variables simultaneously by transforming them into a single desirability score. This method aims to find the most desirable combination of input variables that meet specific

criteria or targets for different responses, allowing for the identification of optimal settings for complex systems or processes (Box et al. 2005).

Table 4.15: Comparison of the experiment and Taguchi method results.

Response variables	Experimental result	Predicted result	Difference (%)
Ultimate tensile strength	32.90 Mpa	35.94 Mpa	9.24
Tensile modulus	920.67 Mpa	996.07 Mpa	8.12
Compressive strength	75.8 Mpa	82.36 Mpa	8.64
Part weight	5.22 g	5.28 g	1.16
Energy consumption	0.02 KWH	0.0211KWH	5.5

The DFA method, a critical criterion for determining process acceptability is the adherence of each response within predefined desired limits. It is to identify an optimal set of parameters that yield the most favorable values for individual response variables. To facilitate this evaluation, all quality characteristics are normalized to a uniform range between 0 and 1, allowing for a consistent comparison (Devarajaiah and Muthumari 2018).

Subsequently, individual desirability indices are computed for each response variable, reflecting how well they align with the desired targets. These indices provide a quantified measure of the desirability of each response. Furthermore, for a comprehensive assessment of the entire process, a weighted geometric mean is employed for each pair of response variables. This calculation yields a composite desirability index, which integrates the importance of multiple response variables into a single metric. The goal is to identify datasets that demonstrate the highest composite desirability. These data sets represent the optimal parameter settings that yield the most desirable quality characteristics under consideration.

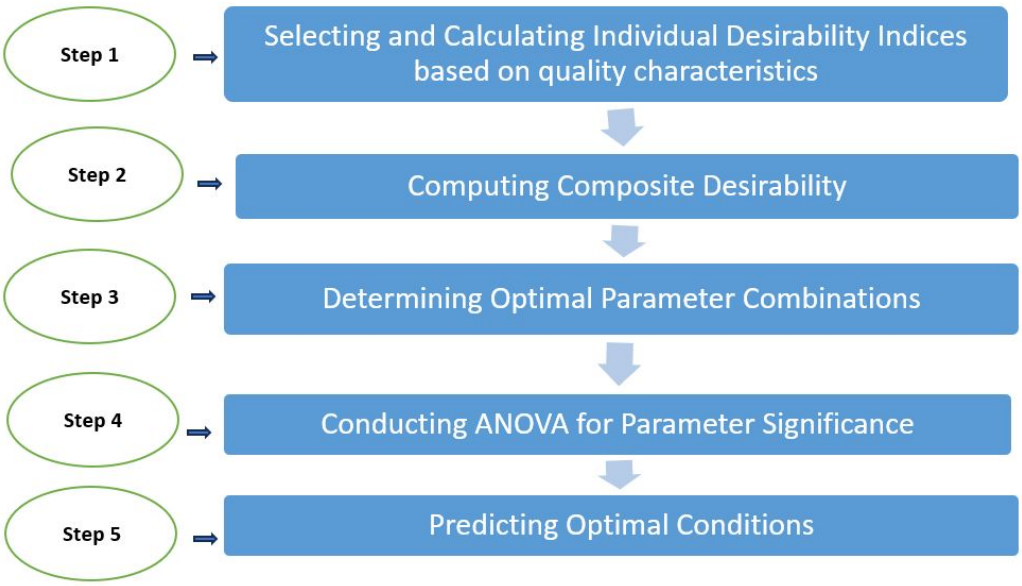

Figure 4.10: Desirability function analysis (DFA) flowchart.

DFA facilitates the identification of process conditions that concurrently optimize multiple responses, ensuring a robust and effective manufacturing process. The optimization process utilizing DFA is illustrated by the flowchart in Figure 4.10. Steps for the procedure of DFA are explained below.

Step 1: The process begins by computing individual desirability indices (d_i) for each response variable. These indices are determined based on specific criteria corresponding to whether each response should be minimized, maximized, or brought to a target value. Desirability functions come in three distinct forms, each fitted with specific response characteristics in accordance with Equations 4.2, 4.3, and 4.4 (Sengottuvel et al. 2013).

i) Nominal - the better characteristics

$$d_i = \begin{cases} \left(\frac{y_r - y_{min}}{Tar - y_{min}}\right)^s, & y_{min} \leqslant y_r \leqslant Tar \\ \left(\frac{y_r - y_{min}}{Tar - y_{min}}\right)^t & T_{ar} \leqslant y_r \leqslant y_{min} \\ 0 & \text{otherwise} \end{cases} \tag{4.2}$$

When a response variable y_r is aimed at achieving a specific target value Tar, the desirability is maximized, reaching a value of 1, precisely when y_r equals Tar. However, if y_r deviates from this target by an extent exceeding a predefined range, the desirability rapidly diminishes to 0. Such a scenario is indicative of an undesirable outcome and is considered the worst-case situation.

ii) Larger -the better characteristics

$$d_i = \begin{cases} 0, & y_r y_{min} \\ (\frac{y_r - y_{min}}{y_{max} - y_{min}})^s, & y_{min} \leqslant y_r \leqslant y_{max},\ s \geq 0 \\ 1 & y_r \geq y_{min} \end{cases} \tag{4.3}$$

where, y_r represents the value being measured, and the criteria value is the threshold that determines whether y_r is acceptable or not. When y_r is greater than or equal to the criteria value, the desirability value is set to 1, indicating that it meets the requirement. If y_r is less than the criteria value, the desirability value is set to 0, indicating that it does not meet the requirement.

iii) Smaller-the better characteristics

$$d_i = \begin{cases} 1, & y_r y_{min} \\ (\frac{y_r - y_{max}}{y_{min} - y_{max}})^s, & y_{min} \leqslant y_r \leqslant y_{max} \\ 0 & y_r \geq y_{min} \end{cases} \tag{4.4}$$

In this study, the smaller the better characteristic is applied to determine the individual desirability values when minimizing the power consumption, material consumption, and printing time. When y_r (the performance metric) is less than a particular criteria value for these factors, the desirability value equals 1. Conversely, the larger the better characteristic is applied to maximize tensile and compressive properties. When y_r exceeds a particular criteria value for tensile and compression, the desirability value equals 1.

Step 2: This step decides the composite desirability (DG) by aggregating the individual desirability indices through weighted averaging as shown in Equation. 4.5.

$$D_G = \sqrt[k]{(d_1^{w_1} \times d_2^{w_2} \ldots d_i^{w_i})} \tag{4.5}$$

Step 3: Determines the most favorable combination of parameters and their respective levels for identifying optimal parameters and levels. The DG serves as a key indicator of product quality.

Step 4: Conducts an Analysis of Variance (ANOVA) for gauging the significance of various parameters. It evaluates the relative importance of each parameter by considering the calculated total sum of squares.

Step 5: The optimal conditions are decided based on the optimal levels for the design parameters, this step calculates and predicts the quality characteristics using the optimal parameters settings. This process ensures that the expected quality is achieved based on the selected parameter configuration.

4.10 Implementation of DFA

The individual desirability values for each response variable are computed by using Equation no. 4.3 and 4.4, the results are listed in Table 4.16. Additionally, the composite desirability values (DG) are determined by Equation. 4.5, with equal weights assigned (0.5) to all parameters. After getting the composite desirability for the response variables, the objective of composite desirability is to select the highest value for the response variables. A set of experiments with the highest composite desirability value is needed to select the parameters level combination to get the optimum result. Settings or levels of input variables are decided to produce the most desirable outcomes across various criteria. Experiments with the highest composite desirability value signify the configuration of input variables that collectively satisfy the desired objectives or criteria to the greatest

extent (Myers et al. 2002). The optimum condition associated with the highest composite desirability in the specified experimental domain is highlighted in bold in Table 4.16. From the selected parameter level combination, the initial optimum parameter settings are obtained. In the further ANOVA analysis, the final optimum parameter level combination is achieved.

Table 4.16: Predicted Desirability Value for the response variables.

Individual desirability									
Sample	Compression	UTS	modulus	Power	scrap	part	Time	CDI	Rank
1	0.81966	0.712588	0.752282	1	0.95399	1	0.917544	0.8607286	9
2	0.901079	0.79826	0.869234	1	0.86576	0.9316	0.933619	0.8827691	7
3	0.975886	0.667209	0.820564	1	0.86576	0.8804	0	0	13
4	0	0.880459	0.902716	1	0.80601	0.9419	0.989679	0	13
5	0.828482	0.914818	0.927137	1	0.97865	0.8736	0.991194	0.8928496	5
6	0.975626	0.810122	0.877884	1	0.80601	0.8422	0.91009	0.873887	8
7	0.640727	0.950231	0.769693	1	0	0.8307	0.980273	0	13
8	0.829192	0.928794	0.953852	1	0.94002	0.8086	0.986604	0.8831731	6
9	0.967332	0.977504	0.97124	1	0.90752	0.5106	0.998565	0.8401664	10
10	0.831994	0	0	1	0.88814	0.9992	0.94414	0	13
11	0.897205	0.870788	0.880743	1	0.92464	0.9298	0.885152	0.9031638	2
12	0.956824	0.850254	0.897738	1	0.94002	0.8528	0.907519	0.9005582	3
13	0.598623	0.861966	0.846869	1	0.94002	0.9489	0.997117	0.8297358	12
14	0.88821	0.831066	0.867159	1	0.98968	0.9015	0.942092	0.8962108	4
15	**1**	**0.985528**	**0.97149**	**1**	**0.92464**	**0.7505**	**0.977011**	**0.9109203**	**1**
16	0.6132	0.972045	0.9557	1	0.88814	0.8377	0.992695	0.8389908	11
17	0.814231	0.927317	0.922949	0	0.94002	0.8042	1	0	13
18	0.963156	1	1	1	1	0	0.97368	0	13

The mean factor effect at each level on Composite Desirability (CD) is calculated and presented in Table 4.17. The influence of these factors on the mean composite desirability is shown in Figure 4.11. The highest mean CD is achieved when wall thickness is set to level 2, layer height is set to level 2, infill density is set to level 3, cubic infill pattern,

printing speed at level 2, and printing temperature at level 1. As a result, the optimal parameter configuration for all the mechanical properties and time, material and energy consumption are determined to be A2B2C2D1E2F1. Further experiments are conducted by utilizing the optimal parameter settings derived from the DFA analysis to assess the improvement in the response variables. The initial and final parameter level combinations are shown in Table 4.18.

Table 4.17: Analysis of Variance (ANOVA) for Composite Desirability.

Source	DF	Seq SS	Adj SS	Adj MS	P
Wall thickness(mm)	1	156.1	156.1	156.1	0.346
Layer height(mm)	2	6854.3	6854.3	3427.2	0.002
Infill density (%)	2	1317	1317	658.5	0.066
Infill Pattern	2	1156	1156	578	0.083
Printing Speed(mm/s)	2	780.3	780.3	390.2	0.153
Printing Temperature (°C)	2	350.3	350.3	175.2	0.372
Residual Error	6	896.4	896.4	149.4	
Total	17	11510.5			

4.11 Optimal level prediction and validation

A2B2C3D1E2F3 is the initial parameter setting that yields the maximum Composite Desirability value shown in Table 4.16. Based on Desirability Function Analysis, A2B2C2D1E2F1 is the ideal parameter configuration. Further experiments are carried out in FDM utilising the input parameters (Wall thickness of 1mm, 0.2 mm layer height, 50% infill density, the cubic infill pattern, printing speed at 75 mm/s and 200℃ printing temperature) that are obtained from the desirability approach, to test the optimal output values of the desirability approach. Response variables such as the printing time, energy consumption, scrap weight, part weight, UTS, tensile modulus and compressive stress

output values are obtained as 43.5 min, 0.06 KWh, 0.09 g,6.97 g, 33.19Mpa, 924.69 MPa and 76.02 MPa, respectively. The desirability approach yields the best outcome for all replies in a single set of input when these values are compared to the individual optimum responses found in the L18 array of tests. The result of validation and improvement in performance measures are presented in Table 4.19.

Table 4.18: Parameter level combination based on DFA.

Initial Parameter level combination	Final Parameter level combination
A2B2C3D1E2F3	A2B2C2D1E2F1
Composite desirability	
0.91	0.93

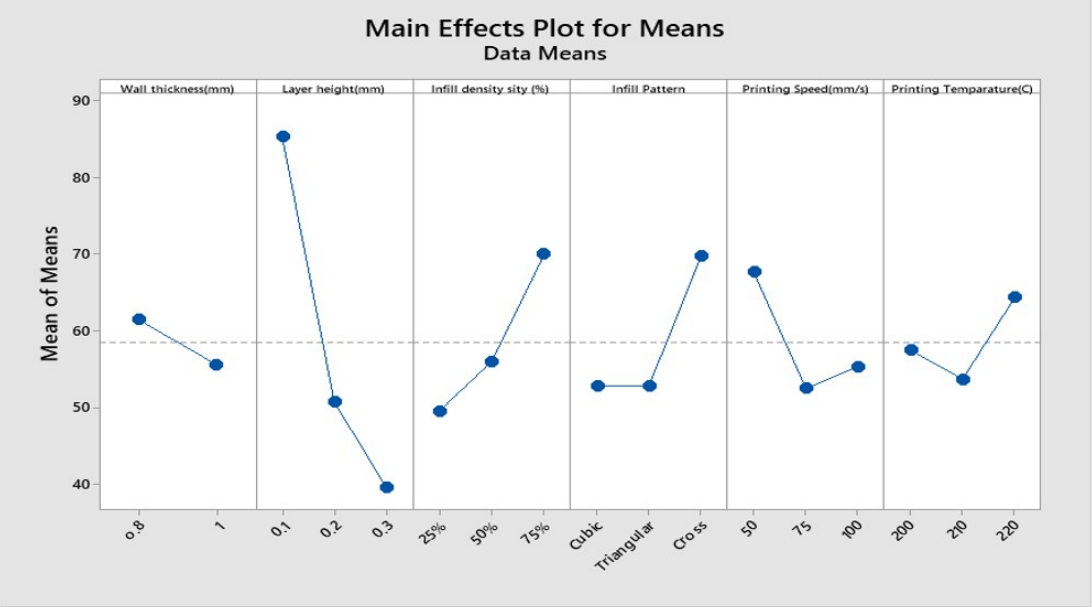

Figure 4.11: Main Effects Plot for Composite Desirability.

Table 4.19: Improvement of response variables.

Initial Parameter level combination (A2B2C3D1E2F3)					
Time	Energy	Scrap weight	Part weight	UTS	Compressive Stress
(min)	(KWh)	(g)	(g)	(MPa)	(MPa)
47	0.07	0.12	8.4	31.12	75.8
Final Parameter level combination (A2B2C2D1E2F1)					
Time	Energy	Scrap weight	Part weight	UTS	Compressive Stress
(min)	(KWh)	(g)	(g)	(MPa)	(MPa)
43.5	0.06	0.09	6.97	33.19	76.02
Improvement (%)					
Time	Energy	Scrap weight	Part weight	UTS	Compressive Stress
(min)	(KWh)	(g)	(g)	(MPa)	(MPa)
7.44%	14.28%	25%	17.02%	6.65%	0.29%

In summary, this chapter provides a thorough statistical analysis of the printed specimens. The experimental procedures and data collecting offer a thorough examination of all the parameters investigated, explaining their importance and influence on the results obtained. The chapter also provides insights into the statistical analysis to evaluate the experimental data using optimization techniques. A particular focus gives on the application of desirability function analysis which is an effective optimization tool to determine ideal parameter configurations to produce desired results.

Chapter 5

Tool Development for Parameter Setting

5.1 Flowchart of the FDM Parameter Setting Tool

A tool is proposed to simplify the complex task of setting parameters for optimal results in FDM. The flowchart of the tool in Figure 5.1 shows steps in configuring and customizing the FDM processing to meet user requirements. It outlines the process sequence of actions in initializing the system for validating user inputs, updating parameter values, saving configurations, and confirming successful updates. It begins with initialization of the FDM system. A database is established using Microsoft Access. The required data are saved in the database. A user interface is created using Visual Basic and linked to the database for user interactions and data administration. The user interface allows users to view and modify parameters. If the inputs are correct, the process progresses to the next step; otherwise, a message will be generated for the user to correct the input.

The user inputs will update parameters in the system to meet user preferences. The updated parameters are saved for future reference. A confirmation message is presented

to the user, indicating the successful parameter settings. The procedure ends with an analysis of outputs in comparison with the predetermined outcomes, ensuring that all goals are attained.

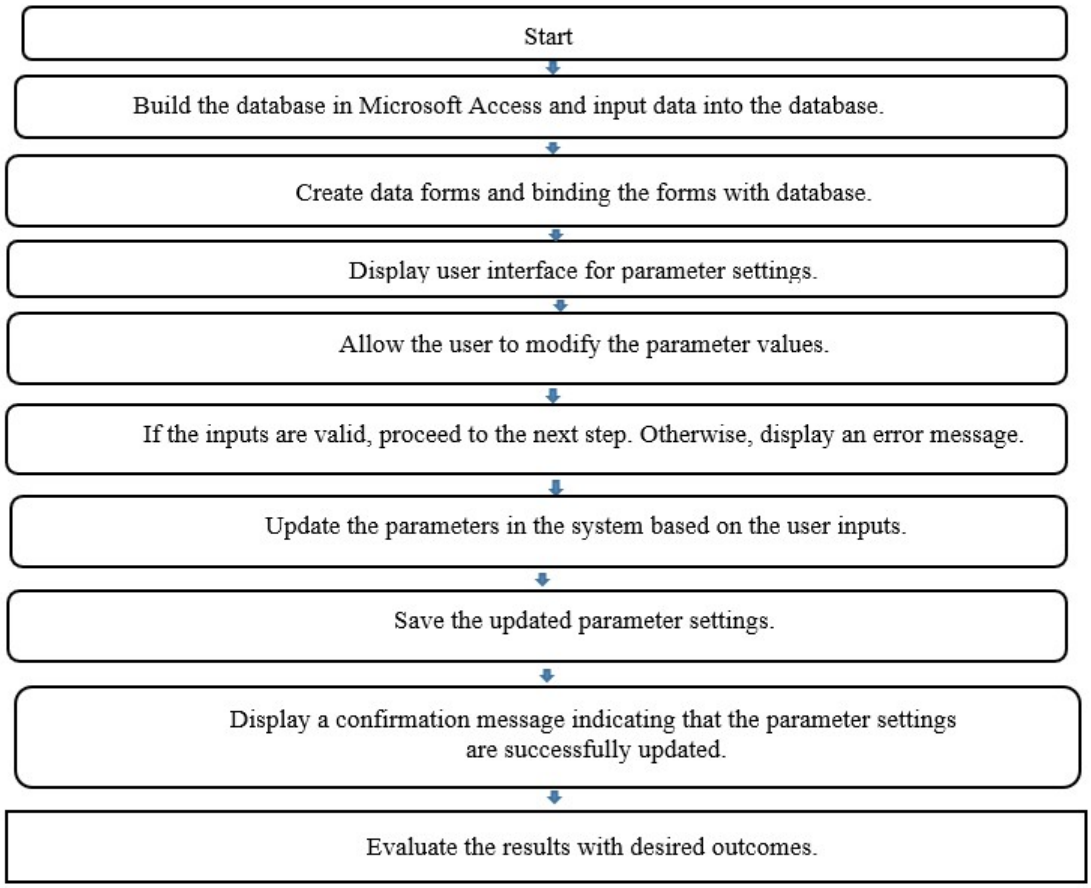

Figure 5.1: Steps of the AM parameter setting tool.

5.2 Design and Implementation of the User Interface for Parameter Settings

A Windows user interface is shown in Figure 5.2. The primary menu form is for users to choose parameters in different levels. Users select parameters from tables on the screen menu. 3D printing parameters setting options include functions of Add, Update, Search,

Delete and View. The menu table is user-friendly for users to enter 3D printing data. The database system saves these entered data so that the user can retrieve them in the future.

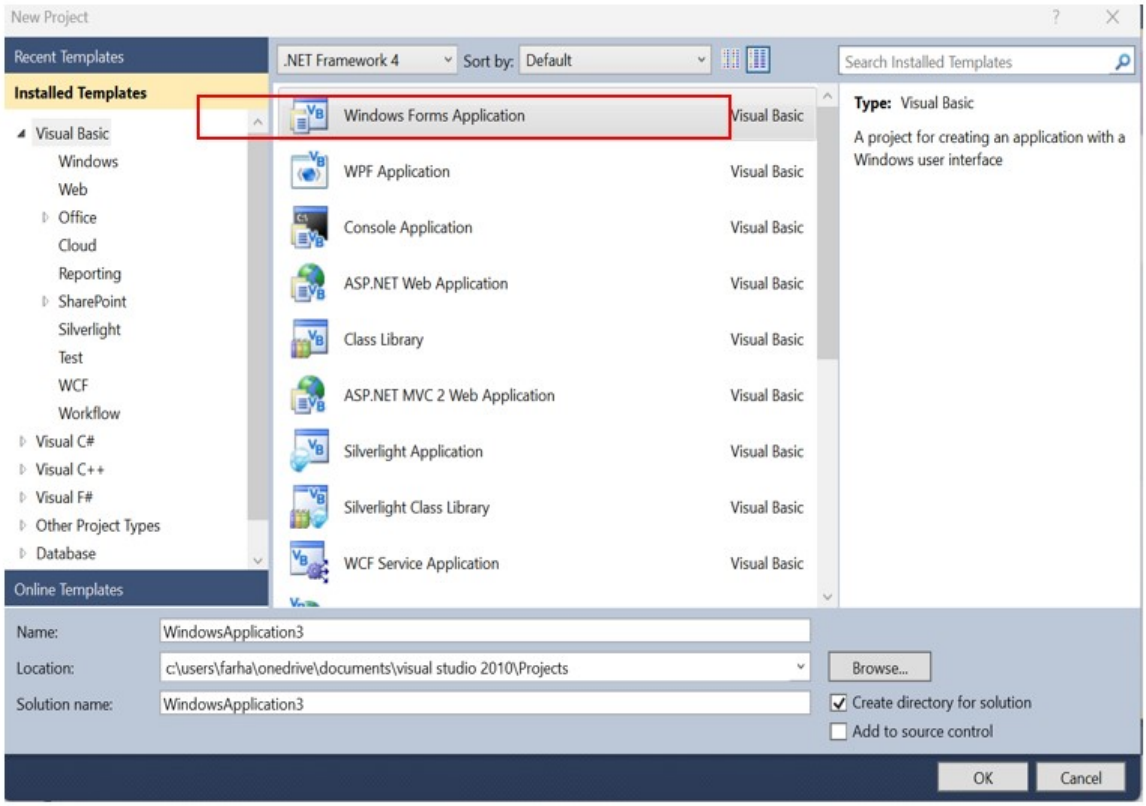

Figure 5.2: User interface.

5.2.1 Program Design

The user interface is built using Visual Basic for users to configure FDM parameters. In the user interface window, users can choose a desired module for execution as shown in Figure 5.2. After the user selection, required forms are created, and linked to the data source for parameter settings. The tool development includes four main steps are as follows.

Step 1: Collecting input data

Data are collected from the results of the work described in previous chapters. They are different parameter combinations of the wall thickness, layer height, infill density, infill pattern, printing speed, and printing temperature in the FDM process. These experimental data are saved in the database. Therefore, Data also include the product name, machine model defined by the user, printing parameters with different levels, printing orientation, etc.

Step 2: Building database in Microsoft Access and saving data in the database

This process builds a database using Microsoft Access to save collected data in the database table as shown in Figure 5.3.

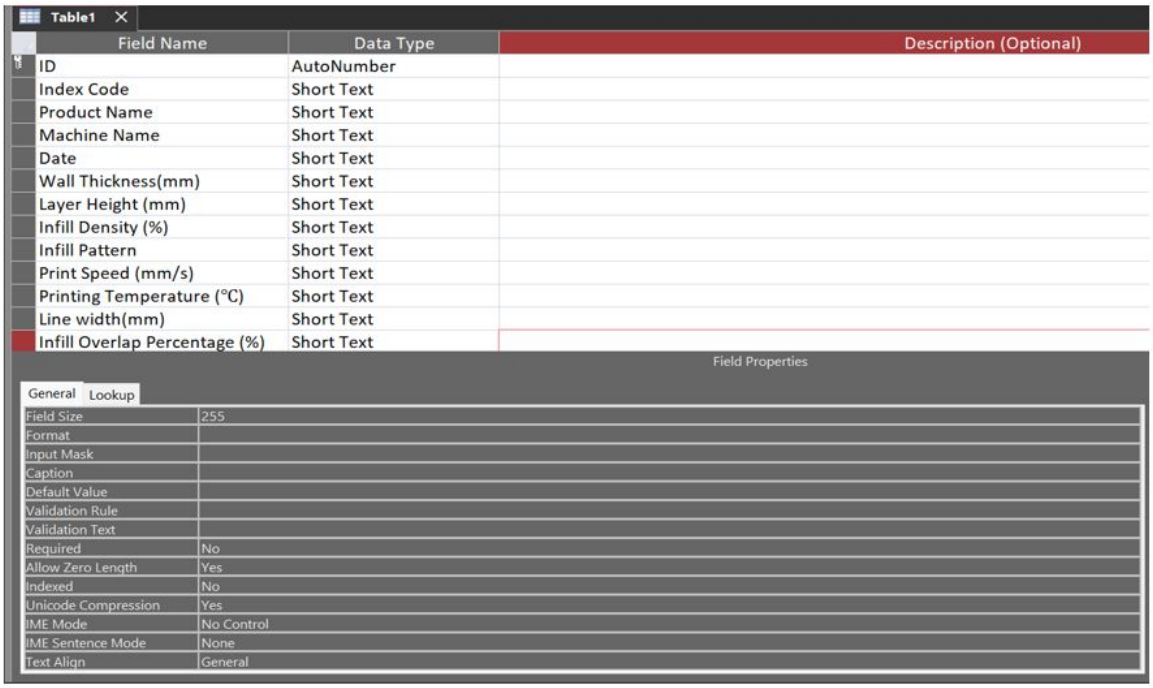

Figure 5.3: Input data into Microsoft Access.

Step 3: Building forms in visual basic and binding the forms with database

Operation forms are built using Visual Basic. The form depicted in Figure 5.4 enables users to work with the database. The next step establishes a link between the database

and forms to ensure that the data can be efficiently accessed, displayed, and modified through the user interface to facilitate data management and customization.

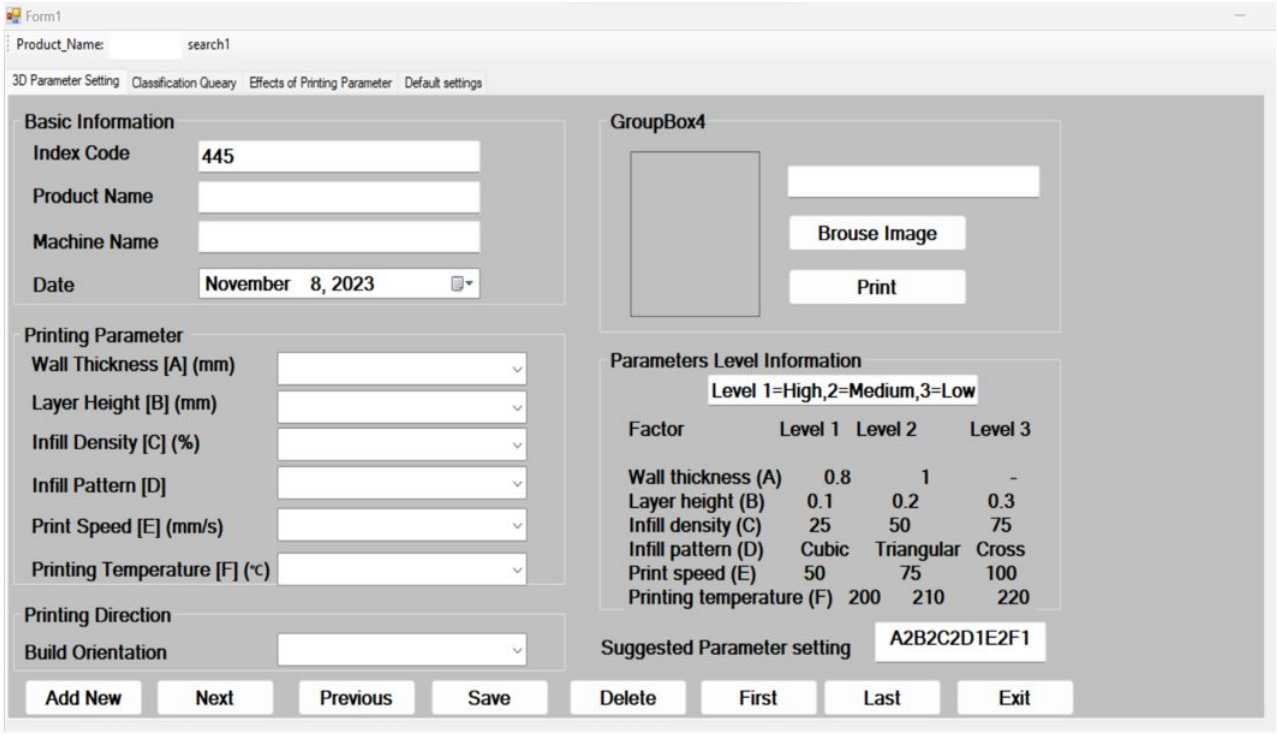

Figure 5.4: Parameter settings user interface form.

Step 4: Testing the program design

The parameter setting is carried out using the process displayed in Figure 5.5. The input is a data file containing the part design and default parameter values. The output is the optimum parameter setting for the FDM process. The procedure includes the following steps.

1) Open the home screen form.

2) Select the data file.

3) Set the range of parameter values. For each parameter, specify the minimum and maximum values.

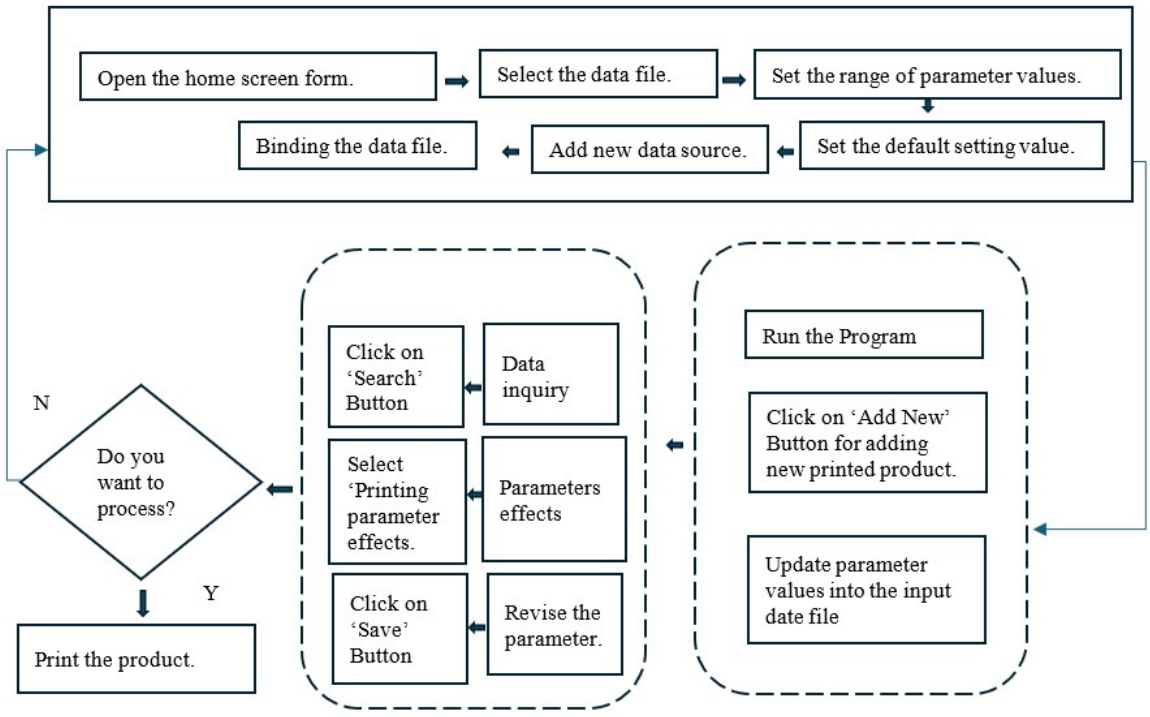

Figure 5.5: Diagram to determine the parameter settings for FDM process.

4) Click the Run Program button.

5) The program will bind the data file, add a new data source, and set the default setting value.

6) Click the 'Search' Inquiry button. The program will calculate the parameter effects for each parameter combination within the specified range

7) Review the parameter effects.

8) If the user wants to know the parameter effects, click the 'Printing Parameter Effects' button. The program will update the new parameter values in the input data file.

9) Click the 'Save' button to save the updated data file.

10) Click the Print the Product button to print the part.

11) If the user is not satisfied with the parameter effects, the parameter values can be revised to repeat steps 5-8.

5.3 Program Implementation

The program starts by displaying a main settings form, it is a four-tab page including a 3D parameter settings Tab, a Classification Queary Tab, an Effects of Printing Parameters Tab, and a Default settings Tab, where the user can select any of the Tabs according to the need for searching or adding new data items. Its structural process is shown in Figure 5.6.

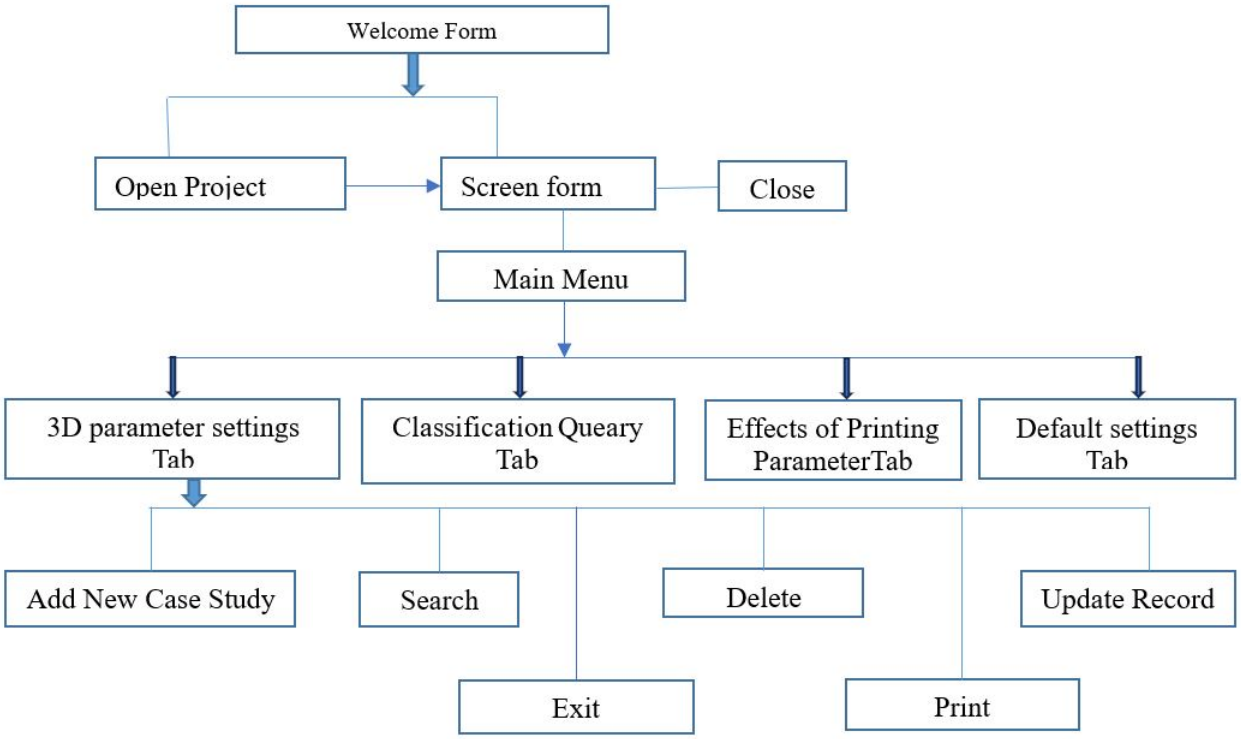

Figure 5.6: Structural process of user interface tool.

The user data can be added, deleted, changed, sorted, or searched using the database management system. The connection between the data source and user interface is built using the Data Source Configuration Wizard as shown in Figure 5.7. Once the data

source is linked to the user interface, the data are saved in Microsoft Access database files. Figure 5.8 represents the saved data file from previous 3D-printed samples. Figures 5.9 and 5.10 show the program implementation by adding new case parameter settings in the database and searching information from the database system.

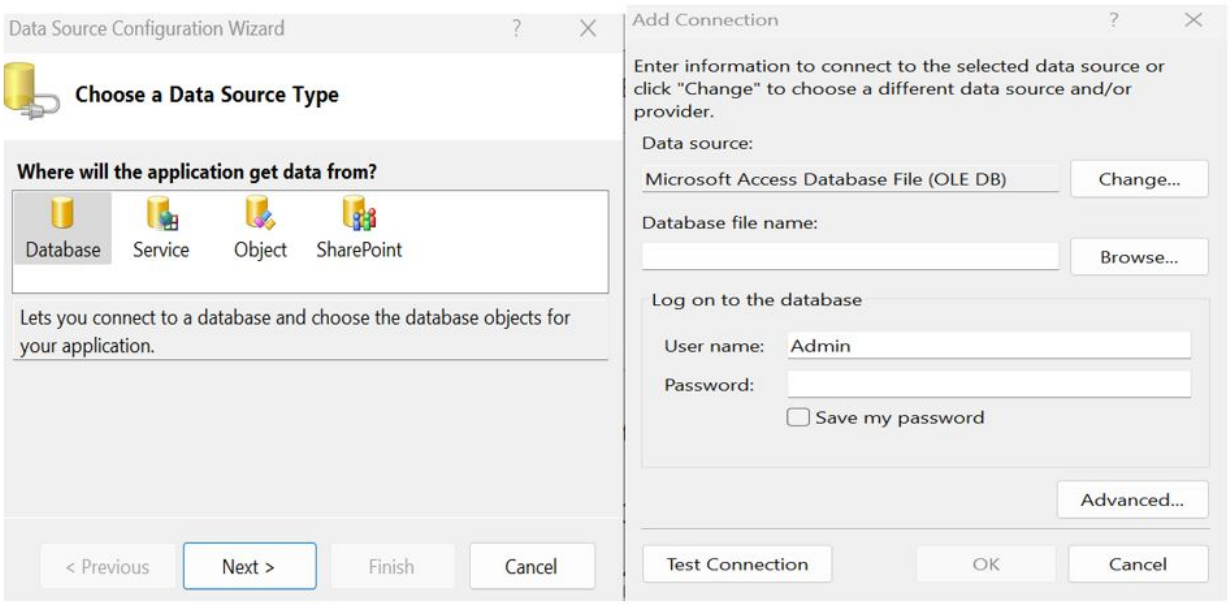

Figure 5.7: Data source connection.

Table1

ID	Index Code	Product Nam	Machine Na	Date	Wall Thickne	Layer Height	Infill Density	Infill Pattern	Print Speed (	Printing Tem	Line width(n
1	445										
2	119	Toy car	Creality 3	August 7,2023	0.8	1.0	75	Cross	100	220	0.4
3	127	toy ball	Cube pro	August 7,2023	1.0	1.0	25	Cubic	50	200	0.4
4	008	boat fin	Ender	August 9,2023	1.0	0.2	50	Triangular	75	210	0.4
5	556	box holder	Cube pro	August 19,2023	1.0	0.2	50	Cubic	75	200	0.4
6	001	Air gun	Creality 3	September 1, 2	1.0	0.2	50	Cubic	75	200	0.4
7	002	box with lids	Ender3	September 5, 2	1.0	0.2	50	Triangular	75	210	0.4
8	003	hook	Creality	September 6, 2	0.8	0.2	50	Triangular	75	210	0.4
9	004	Cookie cutter	Creality	September 4, 2	1.0	0.2	50	Triangular	75	210	0.4
10	005	Key hanger	Ender3	September 3, 2	1.0	0.2	50	Cubic	75	200	0.4
11	115	Page holder	Ender 3	October 16, 20	0.8	0.2	25	On edge	75	210	4%
12	115										
(New)											

Figure 5.8: Stored data in Microsoft Access database file.

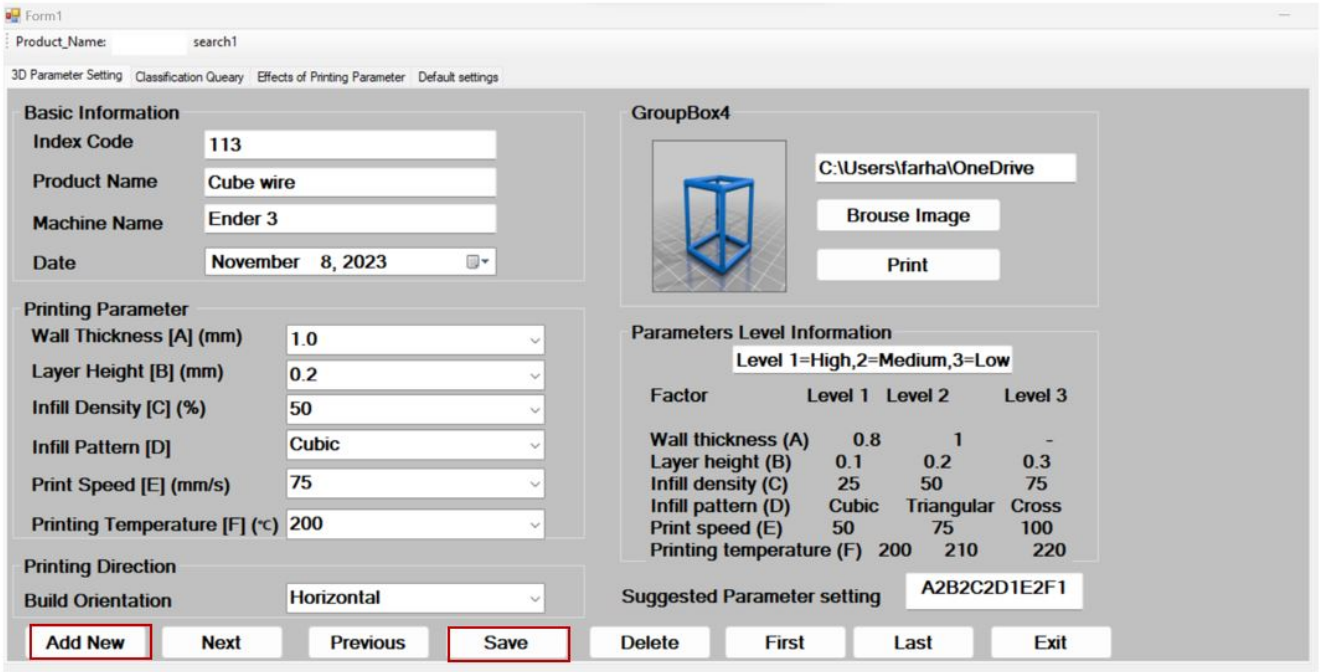

Figure 5.9: The result after debugging the program.

5.4 Case Study

A 3D printing case study is used to demonstrate the tool application to reduce the failure rate, improve the overall printing quality and time, and quickly choose the best parameters for the printing process. A wire headphone organizer is selected for printing. Figure 5.11 shows parameter settings displays all the information of related to the case study, including the product name, index code, printing parameter settings, print object image, problems that can occur during printing, and techniques to correct the flaws with the help of the "Effect of printing Parameter" tab. Additionally, users can efficiently retain the parameter settings for future use by simply utilizing the save function. Subsequently, Figure 5.12 shows the resultant printed output. This case study demonstrates the developed tool in optimal printing parameters, reducing printing time, and ensuring the quality of the printed product.

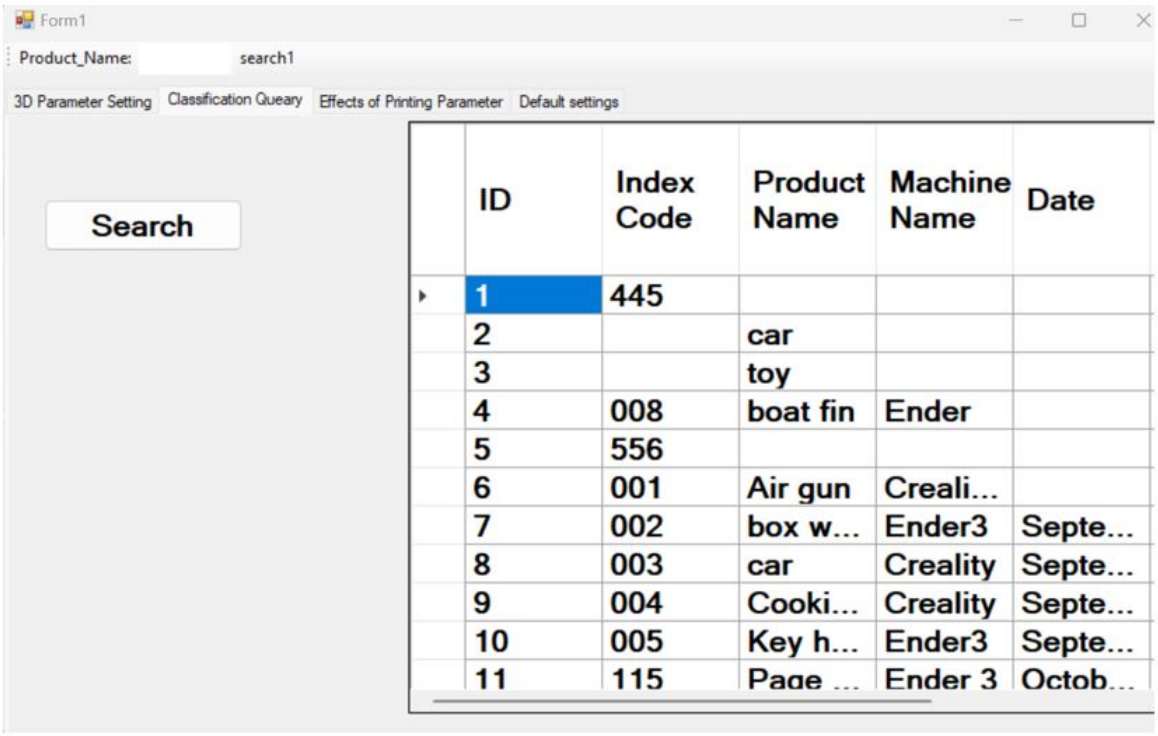

Figure 5.10: Search information from previously saved data.

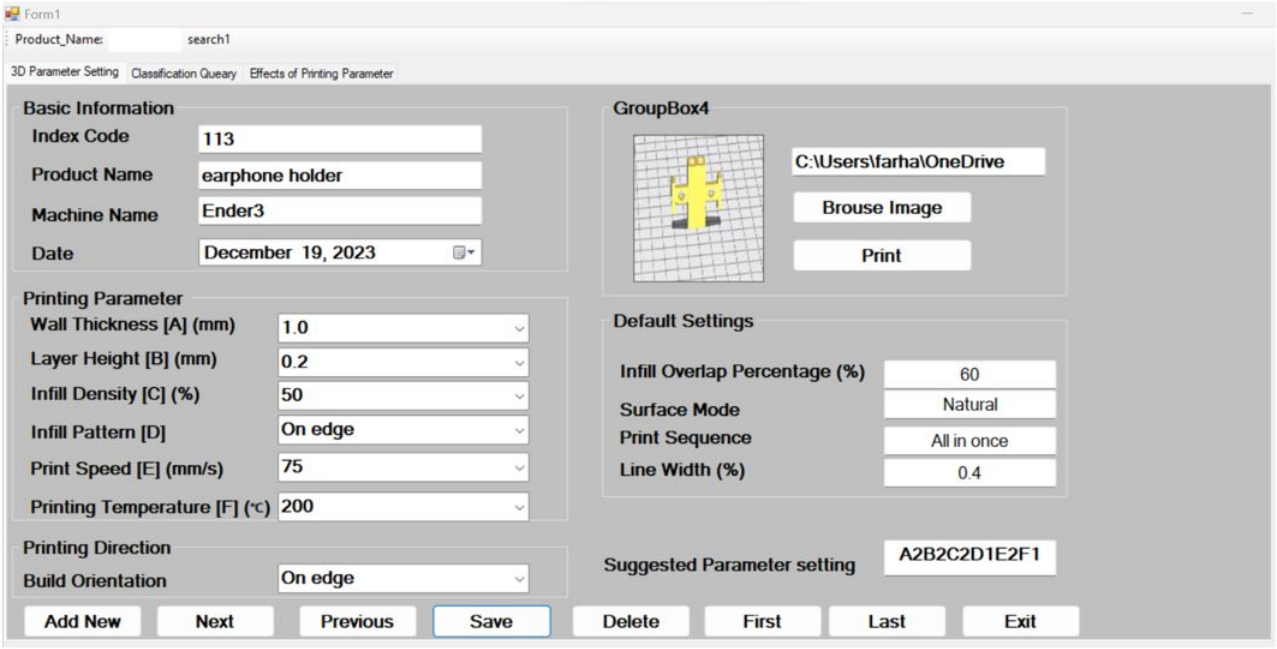

Figure 5.11: Case study parameter settings Tab.

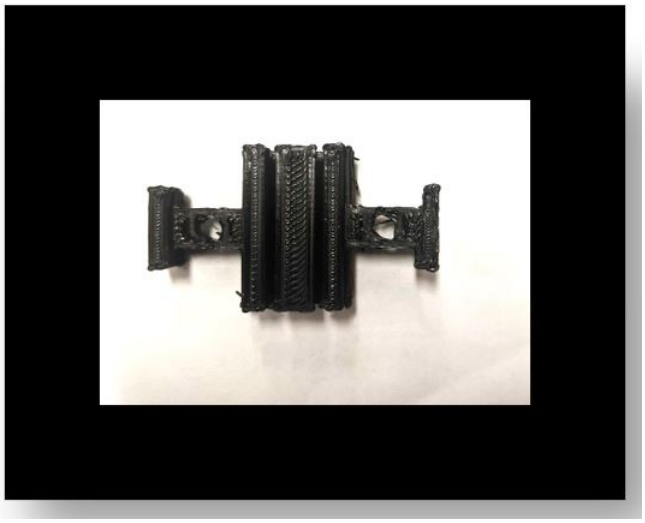

Figure 5.12: Printed product.

The system can add new cases into the case library to expand the database. Based on our research, six setup parameters are chosen in the tool. It is possible to define additional characteristics for the parameters, such as the orientation angle, style of the top, and bottom, printing plane, and table position. These parameters are fixed in the developed tool for user references as most cases are unlikely to alter these attributes.

In summary, this chapter introduces the tool development in creating a user interface for configuring 3D printing parameters. It outlines steps in developing the user interface, including the creation of the structure and functionality of the interface. It further discusses the implementation of the user interface. The chapter also addresses the practical application of the interface in setting up 3D printing parameters in a case study.

Chapter 6

Conclusion and future work

This research examines six parameters in Fused Deposition Modeling of the 3D printing process, denoted as wall thickness, layer height, infill density, infill pattern, printing speed, and printing temperature, at two and 3 mixed level settings in fabricating test parts. Utilizing a fractional factorial design, an extensive experimentation plan is implemented to ascertain the parameter configurations that influence specific output characteristics outlined. The Taguchi DOE approach is used to determine the optimal FDM process parameters and examine the impact of various process variables on 3D-printed parts. The FDM technology is used to build 18 samples by different parameter combinations of the selected six control factors in the 3D printing process. The greater-better criterion is used to examine the S/N ratio of the mechanical qualities of tested samples. A lower S/N ratio is utilized for analyzing the printing time, energy utilization, and material quantity. Based on the Taguchi S/N ratio analysis, the ideal condition for the best performance of the printed parts is identified. Although the modulus of elasticity shows slight variations from the tensile strength in different parameters, it discovers that the layer height is the most important parameter among all the selected six parameters on the response variables except the compressive stress. The infill density has the highest impact on compressive stress. The layer height is the second most impact parameter. By using

the Taguchi S/N ratio analysis, the best parameter level combination of parameters is found for all the responses. The ANOVA and contribution analysis are used to identify percentages of parameter contributions to the responses. After conducting the desirability function analysis, the optimal parameter configuration for optimizing all the mechanical properties and time, material, and energy consumption is determined as A2B2C2D1E2F1. The Taguchi design approach and experimental results match well for the solutions. The following settings are suggested for fabricating FDM parts:

- Using layer height at 0.2 mm, cross infill pattern, and least infill density can reduce the material used.
- Least printing time can be achieved when using the 25% infill density, 100 mm/s printing speed, maximum layer height, and cubic filling pattern.
- The layer height and printing speed have significant effects on energy usage.
- Layer height has the biggest impact on both tensile strength and tensile modulus.
- Infill density has the biggest impact on compressive stress. The layer height and printing speed also impacts the compressive stress.

6.1 Research Contributions

This research provides useful information for industrial enterprises to effectively use FDM in AM. To minimize the AM lead time and maximize productivity, this study investigates parameters of the FDM process. Sustainable production is characterized by the low energy use and short production time. The longer the time, the more energy the 3D printer uses and the human resources required for the operation. Sustainability is improved from economic and environmental standpoints by reducing energy and material usage. With the

influence of parameter settings for lowering the process energy and material consumption to increase the sustainability. The suggested method can be adaptable to a variety of AM processes.

6.2 Limitation and Recommendations for Future Research

The limitation of this research is the use of simple and small numbers of specimens. The carbon emission analysis is excluded. The method solution depends on the process of the simulation and experiment used to determine the impact of the process parameters. Different material samples and AM processes should be considered for more general solutions. There are also different printing parameters to affect the result, such as the nozzle diameter, nozzle temperature, print bed temperature, and raster angle. Using a range of angles to optimize the raster orientation parameter may help reduce stress in particular areas of an FDM product. These limitations will be improved in our further research.

Bibliography

Ahn, D.-G. (2016). Direct metal additive manufacturing processes and their sustainable applications for green technology:A review. *International Journal of Precision Engineering and Manufacturing-Green Technology*, 3:381–395. https://doi.org/10.1007/s40684-016-0048-9.

Akhoundi, B., Eshraghi, S., and Rafiee, R. (2019). Investigating the mechanical properties of additive manufacturing PLA parts. *Rapid Prototyping Journal*, 5:958–967.

Alhubail, M. (2012). *Statistical-based optimization of process parameters of fused deposition modelling for improved quality*. PhD thesis, University of Portsmouth.

Armstrong, M., Mehrabi, H., and Naveed, N. (2022). An overview of modern metal additive manufacturing technology. *Journal of Manufacturing Processes*, 84:1001–1029. https://doi.org/10.1016/j.jmapro.2022.10.060.

ASTM (1898). ASTM international. https://www.astm.org/.

ASTM-D638-14 (2022). Standard test method for Tensile properties of plastics ASTM D638 - 14: Standard test method for tensile properties of plastics. https://www.astm.org/Standards/D638.htm. 20.07.2022.

ASTM-D638-22 (2022). Standard test method for tensile properties of plastics. https://www.astm.org/d0638-22.html. 18.07.2022.

ASTM-D695-23 (2023). Standard test method for compressive properties of rigid plastics. https://www.astm.org/d0695-23.html.

Berman, B. (2012). 3-D printing: The new industrial revolution. *Business horizons*, 55(2):155–162. https://doi.org/10.1016/j.bushor.2011.11.003.

Blakey-Milner, B., Gradl, P., Snedden, G., Brooks, M., Pitot, J., Lopez, E., Leary, M., Berto, F., and Du Plessis, A. (2021). Metal additive manufacturing in aerospace: A review. *Materials & Design*, 209:110008. https://doi.org/10.1016/j.matdes.2021.110008.

Box, G. E., Hunter, J. S., and Hunter, W. G. (2005). Statistics for experimenters. In *Wiley series in probability and statistics*. Wiley Hoboken, NJ.

Campbell, I., Bourell, D., and Gibson, I. (2012). Additive manufacturing: rapid prototyping comes of age. *Rapid prototyping journal*, 18(4):255–258. https://doi.org/10.1108/13552541211231563.

Cavallo, C. (2023). All about Fused Deposition Modeling. https://www.thomasnet.com/articles/custommanufacturingfabricating/fuseddepositionmodeling3dprinting/.

Cuan-Urquizo, E., Barocio, E., Tejada-Ortigoza, V., Pipes, R. B., Rodriguez, C. A., and Roman-Flores, A. (2019). Characterization of the mechanical properties of FFF structures and materials: A review on the experimental, computational and theoretical approaches. *Materials*, 12(6):895. https://doi.org/10.3390/ma12060895.

Dakshinamurthy, D. and Gupta, S. (2018). A study on the influence of process parameters on the viscoelastic properties of ABS components manufactured by FDM process.

Journal of The Institution of Engineers (India): Series C, 99:133–138. https://doi.org/10.1007/s40032-016-0324-z.

Davis, R. and John, P. (2018). Application of Taguchi-based design of experiments for industrial chemical processes. *Statistical approaches with emphasis on design of experiments applied to chemical processes*, 137. https://doi.org/10.5772/intechopen.69501.

Dev, S. and Srivastava, R. (2020). Experimental investigation and optimization of FDM process parameters for material and mechanical strength. *Materials Today: Proceedings*, 26:1995–1999. https://doi.org/10.1016/j.matpr.2020.02.435.

Devarajaiah, D. and Muthumari, C. (2018). Evaluation of power consumption and MRR in WEDM of Ti–6Al–4V alloy and its simultaneous optimization for sustainable production. *Journal of the Brazilian Society of Mechanical Sciences and Engineering*, 40:1–18. https://doi.org/10.1007/s40430-018-1318-y.

Dolata, A. J., Mróz, M., Dyzia, M., and Jacek-Burek, M. (2020). Scratch testing of AlSi12/SiCp composite layer with high share of reinforcing phase formed in the centrifugal casting process. *Materials*, 13(7):1685. https://doi.org/10.3390/ma13071685.

D'Addona, D., Raykar, S. J., Singh, D., and Kramar, D. (2021). Multi objective optimization of fused deposition modeling process parameters with Desirability Function. *Procedia CIRP*, 99:707–710. https://doi.org/10.1016/j.procir.2021.03.117.

Elasha, F. and Masood, S. H. (2020). Application of design of experiments (DOE) methodology for process parameters optimization in additive manufacturing. *The International Journal of Advanced Manufacturing Technology*, 106(3–4):1391–1409. https://doi.org/10.1007/s00170-019-04653-4.

Farahin, K., Farizuan, M., and Radhwan, H. (2019). Analysis performance on original wing 2 HLK168 drone controller using DFMA approach. In *AIP Conference Proceedings*, volume 2129. AIP Publishing. https://doi.org/10.1063/1.5118168.

Gibson, I. (2015). Additive manufacturing technologies 3D printing, rapid prototyping, and direct digital manufacturing. https://doi.org/10.1007/978-1-4939-2113-3.

Gohil, S., Patel, D., and Ramakrishnan, N. (2019). Optimization of process parameters for fused deposition modelling using Desirability Function Analysis. *Materials Today: Proceedings*, 17:1366–1373. https://doi.org/10.1016/j.matpr.2021.02.809.

Gregorian, A., Elliott, B., Navarro, R., Ochoa, F., Singh, H., Monge, E., Foyos, J., Noorani, R., Fritz, B., and Jayanthi, S. (2001). Accuracy improvement in rapid prototyping machine (FDM-1650). In *2001 International Solid Freeform Fabrication Symposium*. https://utw10945.utweb.utexas.edu/Manuscripts/2001/2001-10-Gregorian,Noorani.pdf.

Griffiths, C. A., Howarth, J., De Almeida-Rowbotham, G., and Rees, A. (2016). A design of experiments approach to optimise tensile and notched bending properties of fused deposition modelling parts. *Proceedings of the institution of mechanical engineers, Part B: Journal of Engineering Manufacture*, 230(8):1502–1512. https://doi.org/10.1177/0954405416640182.

Harrington, J. (2006). Practical optimization methods: With Mathematica® Applications. *Materials Research Express*.

Hassanifard, S. and Hashemi, S. M. (2020). On the strain-life fatigue parameters of additive manufactured plastic materials through fused filament fabrication process. *Additive Manufacturing*, 32:100973. https://doi.org/10.1016/j.addma.2019.100973.

Heidari-Rarani, M., Ezati, N., Sadeghi, P., and Badrossamay, M. (2022). Optimization of FDM process parameters for tensile properties of polylactic acid specimens using Taguchi design of experiment method. *Journal of Thermoplastic Composite Materials*, 35(12):2435–2452. https://doi.org/10.1177/0892705720964560.

Huang, B., Shi, L., Zhang, Z., Wang, Y., and Zeng, W. (2018). Influence of process parameters on Tensile properties of ABS parts fabricated by FDM: Experimental and theoretical analysis. *Journal of Materials Processing Technology*, 255:, 536–545.

Huynh, H. N., Nguyen, A. T., Ha, N. L., and Thai, T. T. H. (2017). Application of fuzzy Taguchi method to improve the dimensional accuracy of fused deposition modeling processed product. In *2017 International Conference on System Science and Engineering (ICSSE)*. https://doi.org/10.1109/ICSSE.2017.8030847.

ISO, I. (2015). Standard terminology for Additive manufacturing–General principles–terminology. *ASTM International*.

Ituarte, I. F., Coatanea, E., Salmi, M., Tuomi, J., and Partanen, J. (2015). Additive manufacturing in production: a study case applying technical requirements. *Physics Procedia*, 78:357–366. https://doi.org/10.1016/j.phpro.2015.11.050.

Jamróz, W., Szafraniec, J., Kurek, M., and Jachowicz, R. (2018). 3D printing in pharmaceutical and medical applications–recent achievements and challenges. *Pharmaceutical research*, 35:1–22. https://doi.org/10.1007/s11095-018-2454-x.

Kacker, R. N., Lagergren, E. S., and Filliben, J. J. (1991). Taguchi's orthogonal arrays are classical designs of experiments. *Journal of research of the National Institute of Standards and Technology*, 96(5):577. https://doi.org/10.6028/jres.096.034.

Khalid, M. and Peng, Q. (2021). Investigation of additive manufacturing process parameters for sustainability to optimize energy and material consumption. *Journal of Mechanical Design*, 143(3):032001. https://doi.org/10.1115/1.4049521.

Kruth, J.-P., Leu, M.-C., and Nakagawa, T. (1998). Progress in additive manufacturing and rapid prototyping. *Cirp Annals*, 47(2):525–540. https://doi.org/10.1016/S0007-8506(07)63240-5.

Kusumaatmaja, A., Yusuf, A., and Tarigan, B. (2013). Development of carbon fiber reinforced PLA filament for fused filament fabrication additive manufacturing. *Materials Research Express*, 5(7):e59840.

Lin, T. and Chananda, B. (2003). Quality improvement of an injection-molded product using design of experiments: a case study. *Quality Engineering*, 16(1):99–104. https://doi.org/10.1081/QEN-120020776.

Linke, R. (2017). Additive manufacturing, explained. https://mitsloan.mit.edu/ideas-made-to-matter/additive-manufacturing-explained.

Liu, C., Hu, X., Zhao, Z., and Huang, G. (2020). Optimization of process parameters for selective laser melting using a desirability function approach. materials. *Materials*, 13(7):1685. https://doi.org/10.3390/ma13071685.

May, V. (2022). The history of additive manufacturing: From the 1980s to today.

Melgoza, L., E., Vallicrosa, G., Sereno, L., Ciurana, J., and Rodriguez, C. A. (2014). Rapid tooling using 3D printing system for manufacturing of customized tracheal stent. *Rapid Prototyping Journal*, 20(1):2–12. https://doi.org/10.1108/RPJ-01-2012-0003.

Mohan, N., Senthil, P., Vinodh, S., and Jayanth, N. (2017). A review on composite materials and process parameters optimisation for the fused deposition modelling

process. *Virtual and Physical Prototyping*, 12(1):47–59. https://doi.org/10.1080/17452759.2016.1274490.

Montgomery, D. (2017). *Design and analysis of experiments*. John wiley & sons.

Moon, S. J.and Kim, J. K. N. (2018). The effect of printing orientation on tensile strength in fused deposition modeling. *Metals*, 11(8):877.

Myers, R., Montgomery, D., and Anderson-Cook, C. (2002). Process and product optimization using designed experiments. *Response surface methodology*, 2:328–335.

Ngo, T., Kashani, A., Imbalzano, G., Nguyen, K., and Hui, D. (2018). Additive manufacturing (3D printing): A review of materials, methods, applications and challenges. *Composites Part B: Engineering*, 143:172–196. https://doi.org/10.1016/j.compositesb.2018.02.012.

Nguyen, V., Huynh, T., Nguyen, T., and Tran, T. (2020). Single and multi-objective optimization of processing parameters for fused deposition modeling in 3D printing technology. *International Journal of Automotive and Mechanical Engineering*, 17(1):7542–7551. https://doi.org/10.15282/ijame.17.1.2020.03.0558.

Peace, G. S. (1993). *Taguchi methods: a hands-on approach*. Addison-Wesley.

Popescu, D., Zapciu, A., Amza, C., Baciu, F., and Marinescu, R. (2018). FDM process parameters influence over the mechanical properties of polymer specimens: A review. *Polymer Testing*, 69:157–166. https://doi.org/10.1016/j.polymertesting.2018.05.020.

Profozich, G. (2021). Metal additive manufacturing: What you need to know. https://www.cmtc.com/blog/metaladditivemanufacturingwhatyouneedtoknow.

Qattawi, A., Alrawi, B., and Guzman, A. (2017). Experimental optimization of fused deposition modelling processing parameters: a design-for-manufacturing approach. *Procedia Manufacturing*, 10:791–803. https://doi.org/10.1016/j.promfg.2017.07.079.

Raut, S., Jatti, V., Khedkar, N., and Singh, T. (2014). Investigation of the effect of built orientation on mechanical properties and total cost of FDM parts. *Procedia materials science*, 6:1625–1630. https://doi.org/10.1016/j.mspro.2014.07.146.

Rejeski, D., Zhao, F., and Huang, Y. (2018). Research needs and recommendations on environmental implications of additive manufacturing. *Additive Manufacturing*, 19:21–28. https://doi.org/10.1016/j.addma.2017.10.019.

Rosen, D. (2007). Computer-aided design for additive manufacturing of cellular structures. *Computer-Aided Design and Applications*, 4(5):585–594. https://doi.org/10.1080/16864360.2007.10738493.

Rouf, S., Malik, A., Singh, N., Raina, A., Naveed, N., Siddiqui, I., and Haq, M. (2022). Additive manufacturing technologies: Industrial and medical applications. *Sustainable Operations and Computers*, 3:258–274. https://doi.org/10.1016/j.susoc.2022.05.001.

Roy, R. (2010). *A primer on the Taguchi method*. Society of Manufacturing Engineers.

Ryan, B. (2023). Two-step optimization for Taguchi designs.

Samykano, M., Selvamani, S., Kadirgama, K., Ngui, W., Kanagaraj, G., and Sudhakar, K. (2019). Mechanical property of fdm printed ABS: influence of printing parameters. *The International Journal of Advanced Manufacturing Technology*, 102:2779–2796. https://doi.org/10.1007/s00170-019-03313-0.

Selvaraj, S., Reny, R., and Madhumitha, R. (2021). Experimental evaluation of finding optimum process parameters for aluminium filled PLA material using locally assembled fused filament fabrication printer. 8(7):146–153.

Sengottuvel, P., Satishkumar, S., and Dinakaran, D. (2013). Optimization of multiple characteristics of EDM parameters based on desirability approach and fuzzy modeling. *Procedia Engineering*, 64:1069–1078. https://doi.org/10.1016/j.proeng.2013.09.185.

Sharma, V., Rana, M., Singh, T., Singh, A., and Chattopadhyay, K. (2021). Multi-response optimization of process parameters using Desirability Function Analysis during machining of EN31 steel under different machining environments. *Materials Today: Proceedings*, 44:3121–3126. https://doi.org/10.1016/j.matpr.2021.02.809.

Srivastava, M. and Rathee, S. (2018). Optimisation of FDM process parameters by Taguchi method for imparting customised properties to components. *Virtual and Physical Prototyping*, 13(3):203–210. https://doi.org/10.1016/j.susoc.2022.05.001.

Standard, A. S. T. M. (2012). Standard terminology for additive manufacturing technologies. *ASTM International F2792-12a,1–9*.

Tammas-Williams, S., Withers, P., Todd, I., and Prangnell, P. (2017). The effect of porosity on the fatigue crack growth mechanisms in an additively manufactured titanium alloy. *Acta Materialia*, 136:352–365.

Tanoto, Y. Y., Anggono, J., Siahaan, I. H., and Budiman, W. (2017). The effect of orientation difference in fused deposition modeling of ABS polymer on the processing time, dimension accuracy, and strength. In *AIP Conference Proceedings*, volume 1788. AIP Publishing. https://doi.org/10.1063/1.4968304.

Triditive (2022). What is additive manufacturing? History and benefits. https://triditive.com/what-is-additive-manufacturing-history-and-benefits. 07.07.2023.

Upcraft, S. and Fletcher, R. (2003). The rapid prototyping technologies. *Assembly Automation*, 23(4):318–330. https://doi.org/10.1108/01445150310698634.

Wang, D., Zeng, K., Qi, M., Wang, Y., and Zhao, X. (2019). Influence of process parameters on the tensile strength of Ti6Al4V fabricated by selective laser melting. *Journal of Materials Research*, 34(14):2493–2501. https://doi.org/10.1007/s40436-022-00389-y.

Wang, S., Ma, Y., Deng, Z., Zhang, S., and Cai, J. (2020). Effects of fused deposition modeling process parameters on tensile, dynamic mechanical properties of 3d printed polylactic acid materials. *Polymer testing*, 86:106483. https://doi.org/10.1016/j.polymertesting.2020.106483.

Wiedemann, B. and Jantzen, H.-A. (1999). Strategies and applications for rapid product and process development in Daimler-Benz AG. *Computers in Industry*, 39(1):11–25. https://doi.org/10.1016/S0166-3615(98)00126-2.

Wiki (2023a). Analysis of variance. https://en.wikipedia.org/wiki/Analysis_of_variance.

Wiki (2023b). Stress strain curve. https://en.wikipedia.org/wiki/Stress%E2%80%93strain_curve.

Wong, K. V. and Hernandez, A. (2012). A review of additive manufacturing. *International scholarly research notices*, 2012. https://doi.org/10.5402/2012/208760.

Yadroitsev, I. and Smurov, I. (2010). Selective laser melting technology: From the

single laser melted track stability to 3D parts of complex shape. *Physics Procedia*, 25(5):551–560.

Yang, C.-J. (2022). Accelerated quality improvement of 3D printed objects based on a case-based reasoning system. *The International Journal of Advanced Manufacturing Technology*, 119(7-8):4599–4612.

Yang, K. and El-Haik, B. (2009). *Design for six sigma: A roadmap for product development*. New York: McGraw-Hill, 2nd edition.

Zaman, U. K. u., Boesch, E., Siadat, A., Rivette, M., and Baqai, A. A. (2019). Impact of fused deposition modeling (FDM) process parameters on strength of built parts using Taguchi's design of experiments. *The international journal of Advanced Manufacturing technology*, 101:1215–1226.

Zhang, C., Anzalone, N. C., Faria, R. P., and Pearce, J. M. (2013). Open-source 3D-printable optics equipment. *PloS one*, 8(3):e59840.

Publication

Publication of this research work

Farhana Yasmin, Mustafa Khan and Qingjin Peng (2024), Optimization of Processing Parameters for 3D Printed Product Using Taguchi Method, Computer-Aided Design and Applications, vol. 21(2), 2024, pp. 281-300.